JOURNAL OF AIRCRAFT
Vol. 44, No. 5, September–October 2007

Preliminary Aerostructural Optimization of a Large Business Jet

P. Piperni,* M. Abdo,† and F. Kafyeke‡
Bombardier Aerospace, Montreal, Quebec H4S 2A9, Canada
and
Askin T. Isikveren§
University of Bristol, Bristol, BS8 1TR England, United Kingdom

DOI: 10.2514/1.26989

An overview of an industrial approach to the aerostructural optimization of a large business jet is presented herein. The optimization methodology is based on the integration of aerodynamic and structural analysis codes that combine computational, analytical, and semi-empirical methods, validated in an aircraft design environment. The aerodynamics subspace is analyzed with a three-dimensional transonic small disturbance code capable of predicting the drag of a complete, trimmed aircraft within engineering accuracy. The design of the wing structure is accomplished using a quasi-analytical method that defines the layout of the ribs and geometry of the spar webs, spar caps, and skin-stringer panels, and predicts the wing flexural properties and weight distribution. In addition, the prediction of operating economics as well as the integrated en route performance is coupled into the scheme by way of fractional change functional transformations. To illustrate the automated design system capabilities, the methodology is applied to the optimization of a large business jet comprising winglets, rear-mounted engines, and a T-tail configuration. The aircraft-level design optimization goal in this instance is to minimize a cost function for a fixed range mission assuming a constant maximum takeoff weight.

Nomenclature

A_{sk}	=	cross-sectional area of skin, in.^{2}
A_{st}	=	cross-sectional area of stiffener, in.^{2}
AR	=	aspect ratio
C_{crew}	=	hourly cost of the flight (and cabin) crew, CU/h
C_D	=	total drag coefficient
C_{fees}	=	landing fee charge based on maximum landing weight, CU/lb
C_{fuel}	=	price of fuel, CU/lb
C_L	=	operating lift coefficient
C_{mnt}	=	time-dependent airframe and engine maintenance cost, CU/h
$C_{mnt\ cyc}$	=	cyclic airframe maintenance cost, CU
$C_{mnt\ eng}$	=	cyclic engine maintenance component that is assumed to have a functional dependency with the engine derate level, CU
E	=	relative or absolute error
f	=	function; substitution parameter in modified integrated range model formulation
g	=	acceleration due to gravity, ft/s^2
H	=	fuel calorific value, Btu/lb
k_{aero}	=	control factor used to regulate the extent of coupling (congruity or otherwise) between high-speed and intermediate-speed aerodynamic efficiency
k_{clb}	=	constant of proportionality required to predict all-up weight at top of climb
k_M	=	empirically derived coefficient used to establish a simplified relationship between overall power plant efficiency and Mach number
k_{res}	=	constant of proportionality establishing linear relationship between fractional change in total reserve fuel and fractional change in zero-fuel weight
L/D	=	lift-to-drag ratio
M	=	Mach number
R	=	range, nm
t	=	time, as in block or flight time, h
V	=	forward speed [(knots, calibrated airspeed (KCAS) or knots, indicated airspeed (KIAS)]
W	=	weight of a given component or assembly, all-up weight, lb
x, y	=	arbitrary independent parameters or design variables
z	=	arbitrary dependent parameters or objective functions
α	=	exponent, flight profile correction coefficient when useful load varies but payload is fixed
Δ	=	incremental value
δ	=	engine derate level
ε	=	exponent, flight profile correction coefficient when zero-fuel weight varies
ζ	=	fraction parameter where given quantity is normalized by takeoff gross weight
η	=	nondimensional lateral distance (orthogonal to longitudinal axis) along wing span
η_e	=	overall power plant efficiency
Θ_{prf}	=	trajectory profile correction coefficient
λ	=	exponent, diversion mission dependent regression coefficient
τ_M	=	correlation coefficient used to establish a simplified relationship between overall power plant efficiency and Mach number
υ_{MTOW}	=	partial fraction parameter used to establish a functional association between fractional change in maximum landing weight and fractional change in maximum takeoff weight
χ	=	partial fraction for fractional change operators

Received 2 August 2006; revision received 19 February 2007; accepted for publication 15 March 2007. Copyright © 2007 by the American Institute of Aeronautics and Astronautics, Inc. All rights reserved. Copies of this paper may be made for personal or internal use, on condition that the copier pay the $10.00 per-copy fee to the Copyright Clearance Center, Inc., 222 Rosewood Drive, Danvers, MA 01923; include the code 0021-8669/07 $10.00 in correspondence with the CCC.

*Group Leader, High-Speed Aerodynamics. Senior Member AIAA.
†Engineering Specialist and Flutter and MDO Integrator, NCAP Technical and Aerodynamics. Member AIAA.
‡Senior Engineering Advisor, Manager Advanced Aerodynamics and Strategic Technology. Associate Fellow AIAA.
§Senior Lecturer in Engineering Design, Department of Aerospace Engineering, Group Lead, Aerospace Vehicle Architecture and Design Integration (AVADI) Research and Teaching Group.

Subscripts

div	=	diversion
flt	=	flight
fuel	=	block (as in block fuel)
hld	=	hold
man	=	block maneuver allowance
MD	=	minimum drag
res	=	reserve, summation of hold, and diversion fuel allowance
rfl	=	release fuel
STR	=	structural empty weight (used in quantifying changes from a reference manufacturer's weight empty)
0	=	seed or starting parameter condition
1	=	new or target parameter condition

Symbols

$\triangleleft$	=	fractional change operator, incremental change in parameter normalized by original value

I. Introduction

OVER the course of the last decade a new mind-set has been influencing aircraft product development, and this philosophy is now pervading all facets of aircraft engineering design. To mitigate technical and financial risks and compress program time lines, there is an increasing need for more sophisticated tools with capabilities for analyzing complex, tightly cross-coupled systems and functions involving a wide range of engineering disciplines. The contemporary design task is to achieve an optimal integration of all components into a high performance, robust, and reliable aircraft, with an emphasis placed on modular system architectures as well as producibility at an affordable cost over the whole aircraft life cycle.

Conceptual and preliminary aircraft design comprises a large number of complex trade studies. Such investigations have traditionally been accomplished using a series of limited semi-empirical relations in combination with experience and judicious use of advanced technology multipliers [1]. Recently, as the technology for midtransonic flight has matured, business aircraft manufacturers have developed faster aircraft for increasingly longer-range missions [2,3], and the development of these advanced business aircraft requires the application of sophisticated interdisciplinary technologies more commonly used on larger transport aircraft.

Today, multidisciplinary design optimization (MDO) has become a discipline in its own right, with hundreds of research papers and a growing recognition of its importance. Kroo and Manning [4] and Allwright [5] provide a comprehensive description of the application of collaborative optimization to aircraft sizing and systems integration.

The objective of reducing the design cycle of an aircraft has led to a major research effort into MDO methods. Sobieski and Haftka [6] as well as Balling and Wilkinson [7] presented some of these methodologies and recent developments. Morris and Gantois [8] described a European Union funded research program into MDO, which involved the majority of the European aircraft industry together with university and research organizations. Van der Velden et al. [9] also developed a successful MDO methodology for the preliminary design of the Airbus A3XX, by integrating the FAME-W weight model from DASA-Airbus (Hamburg) and the Globair aerodynamics model from DASA-Airbus (Bremen) into the POINTER^{TM} MDO framework from Synaps, Inc. (now part of Engineous Software, Inc.).

The untwisted wing of elliptical spanwise chord variation, which is predicted by the lifting-line theory (developed by Prandtl [10]) to generate minimum induced drag for a given lift at all angles of attack, represents one of the earliest optimized wings. In that work Prandtl noted that the minimum induced drag was not necessarily the optimum span load distribution. Jones [11] constrained the root bending moment in his analytical calculations for planar wings. Later, Jones and Lasinski [12] constrained the area under the root bending moment curve (the same approach used by Prandtl cited previously) for wings with winglets. For a fixed wing weight and parasite drag, McGeer [13] used an iterative scheme to find the optimum span load for minimum drag. Craig and McLean [14] introduced fuselage interactions and aeroelastic effects while performing trade studies on wing weight and total drag, including profile drag. The MDO study conducted by Wakayama and Kroo [15] combined the aerodynamics and structures subspaces; however, the span load optimization step was not explicitly addressed.

An MDO study by Iglesias and Mason [16] used a discrete vortex method to calculate optimum span load distributions. Changes in wing induced drag and weight were converted to aircraft total gross weight and fuel weight benefits, so that the span loads that give maximum takeoff gross weight (MTOGW) reduction can be found. However, the study did not include detailed structural analysis with wing deformation aeroelastic effects [17].

Several authors such as Giesing and Wakayama [18] have developed an objective function that is based on relative direct operating costs (DOC) for the MDO of a transport aircraft. Johnson [19] has compared the MDO results of optimizing a subsonic wing using various objective functions including MTOGW, fuel, acquisition costs, and weight-based DOC.

Samareh [20] investigated the suitability of available shape parameterization techniques for multidisciplinary applications of complex configurations and presented a free-form deformation method for aerodynamic shape optimization that reduces the number of design variables by an order of magnitude.

Speed and robustness of the optimization algorithms and the quality of the analysis codes used in the optimization process are major contributors to the success of MDO. In recent years, the development of aerodynamic shape optimization methods based on high-fidelity computational fluid dynamics (CFD) and the control theory approach (Jameson et al. [21]) has become an important topic of research. With the adjoint approach, the necessary gradients are obtained through the solution of an adjoint system of equations of the governing equations of interest. This approach is computationally efficient since the complete gradient is independent of the number of design variables and can be used to incorporate higher-fidelity analysis codes into an MDO exercise. Martins et al. [22] have recently presented a novel coupled-adjoint sensitivity method for aerostructural design optimization.

A Reynolds-averaged Navier–Stokes (RANS) aerodynamic solver has also been used by Chiba et al. [23] and Obayashi et al. [24] to optimize the wing of a proposed transonic regional jet using an adaptive range multi-objective genetic algorithm in collaboration with Mitsubishi Heavy Industries, Ltd.

Many authors including some of the ones cited above have taken the AIAA formal definition of MDO, namely, ". . .technology that synergistically exploits the interaction among disparate disciplines to improve performance, lower cost and lower product design cycle time. . ." as one that is suitably represented by aerostructural optimization. However, the authors of this paper consider that a complete MDO capability for aircraft design is one that addresses most if not all of the 10 constituent subspaces within the aircraft product development problem as shown in Fig. 1. For this reason, although the scope of methods and results to be presented can be categorized as one that would contribute to MDO analyses, the term "aerostructural optimization" (ASO) is preferred.

The traditional approach for sizing and optimizing a wing planform has relied on aircraft synthesis codes that use a database of empirical relations. At the other end of the spectrum, the more recent attempts to solve this problem involve the use of high-fidelity codes coupled to the adjoint method to perform wing planform optimization. However, for the conceptual-preliminary design of an aircraft, given the nature and complexity of the trade studies involved and the dearth of geometric detail that characterizes the process, it is impractical to use high-fidelity methods at this early stage of the design. Moreover, the design of an aircraft cannot be fully optimized with only gradient-based optimization techniques, because it is prone to converge on local minima. Ultimately, a hybrid

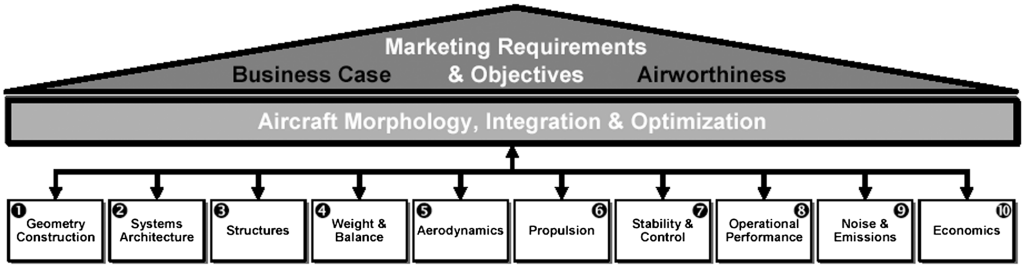

Fig. 1 The complete aircraft product development problem: customer, certification, and integrator requirements transformed into the three macrodisciplines and their associative 10 technical subspaces. Note: manufacturability and producibility consolidated into "Business Case."

strategy is required, wherein each stage and/or subspace of the design process uses the appropriate level of analysis fidelity, coupled to the appropriate type of optimization algorithm.

It is also noted that in practice, the distinction between a "low-fidelity" and "high-fidelity" analysis is not only a matter of the order of the mathematical formulation used, but also the degree to which a code has been calibrated and validated, and the maturity of a given formulation when applied to a large set of complex configurations. The drag of a complete aircraft is predicted routinely in engineering design offices using lower-order formulations that have been enhanced with embedded semi-empirical correlations and calibrated with wind-tunnel testing and validated for a range of aircraft in flight test.

The approach advocated herein is one that separates the design into two stages, that is, a conceptual-preliminary design stage, and a detailed design stage. In the first stage, aircraft-level trade studies are included, and the design space is explored with fast turnaround, lower-fidelity codes linked to optimization algorithms that can handle complex design spaces and overcome local minima. Once a reasonable design is thus achieved, the second stage is executed using high-fidelity codes with gradient-based optimization algorithms.

The objective of this paper is to present an aerostructural optimization methodology suitable for the conceptual-preliminary aircraft design stage in an industrial setting. The aerodynamics subspace is analyzed with a three-dimensional transonic small disturbance (TSD) code capable of predicting the drag of a complete, trimmed aircraft in a fully automated setup in the optimization environment. The structural subspace is analyzed using a quasi-analytical structural design method that can automatically define the internal layout of the ribs, spar webs, spar caps, and skin-stringer panels, and can predict the wing flexural properties and weight distribution, given only the external lines of the wing. The prediction of the other subspace cost functions, such as en route performance and operating economics, is accomplished using fractional change functional transformations derived from an initial reference aircraft candidate. A review of the underlying theory and presentation of a comprehensive validation exercise using fractional change functional transformations can be found in [25]. Validation work has established the applicability of these prediction algorithms for personal/microturbofan aircraft, business aircraft from very light to ultralong range categories, to commercial aircraft from commuters to narrow-body transports of around 100 passengers. The significant features of the abovementioned aerodynamic, structural, integrated performance, and economics analysis methods are described in the sections that follow. Application of the methods to the design of a large business jet configuration is included to illustrate the overall capability.

II. Framework of Aerostructural Optimization Scheme

The industrial design process of a business aircraft is complex in nature and requires the cross-functional interactions of many disciplines including geometry, aerodynamics, structures, weights, performance, and operating economics. The ASO scheme developed in this work (Fig. 2) does not replace the actual design process of a business aircraft; rather, it is seen as assisting the experienced designer in studying a wider class of complex designs in an automated setup.

The present iterative computational procedure has been developed to consider the complete aerodynamic representation of an aircraft including rear-mounted engines, T tail, and winglets. The CFD model of the aircraft is used to generate the cruise and design pressures as well as the aerodynamic forces (lift and drag) and pitching moments. The design shear forces and bending moments are obtained by integrating the aerodynamic loads. In this initial stage of the design process and given only the external aerodynamic shape of the wing, the spanwise weight distribution of the wing is not known. However, the total wing structural weight, which includes the high-lift devices, can be estimated from semi-empirical relationships (general aviation synthesis program, GASP [26]). As a first approximation, the total weight of the wing can then be distributed along the wing span according to the spanwise variation of the wing's local chord length and sectional thickness. The wing spanwise weight distribution is then integrated to yield the inertial shear forces and bending moments. The design loads are then obtained by subtracting the inertial loads from the aerodynamic ones. The next challenging step is to design the wing-box structure given only the external lines of the wing and the design loads. Once the skin-stringer panels, ribs, spars, and spar caps are designed satisfying structural failure modes, the wing-box structural model is then used to calculate wing flexural properties using a program developed in-house called the thin-walled structures analysis program (TWSAP) [27–29]. The wing flexural properties are then used to construct a wing beam finite element model (referred to herein as a wing stick model). The wing structural model (skin thickness and stringer area) is used to obtain a more accurate estimate of the wing weight that is then used to obtain a more refined set of design loads. The wing structure is also linked to the aerodynamic model to calculate wing bending and twisting using NASTRAN [30], as well as the new aerodynamic loads including wing flexibility and load alleviation. These are then used to redesign the structure and obtain a more refined wing weight estimate. During this iterative process, the aerodynamic performance parameters, for example, the lift-to-drag ratio (L/D), and the structural properties are repeatedly used to calculate en route performance characteristics and operating economics. Fuel volume is continuously monitored upon completion of each design iteration to ensure that the wing has enough room to contain the fuel required for the specified aircraft mission.

The multidisciplinary design components and processes are integrated using the iSIGHT^{TM} software (formerly implemented in the EPOGY software from Synaps, Inc., now part of Engineous Software, Inc.). iSIGHT is used to initialize the parameters defining the input and to control the running of the various codes in sequence and in parallel. The design problem needs to be stated in the form of a composite objective function with accompanying design variables and constraints after all the inputs and outputs are defined. iSIGHT provides a variety of optimization and search methods, and the software can also be "trained" to use the most suitable hybrid combination of various optimization algorithms for a given problem.

A description of the aerodynamics, structures, integrated aircraft performance, and economics formulations is given in more detail in the following sections.

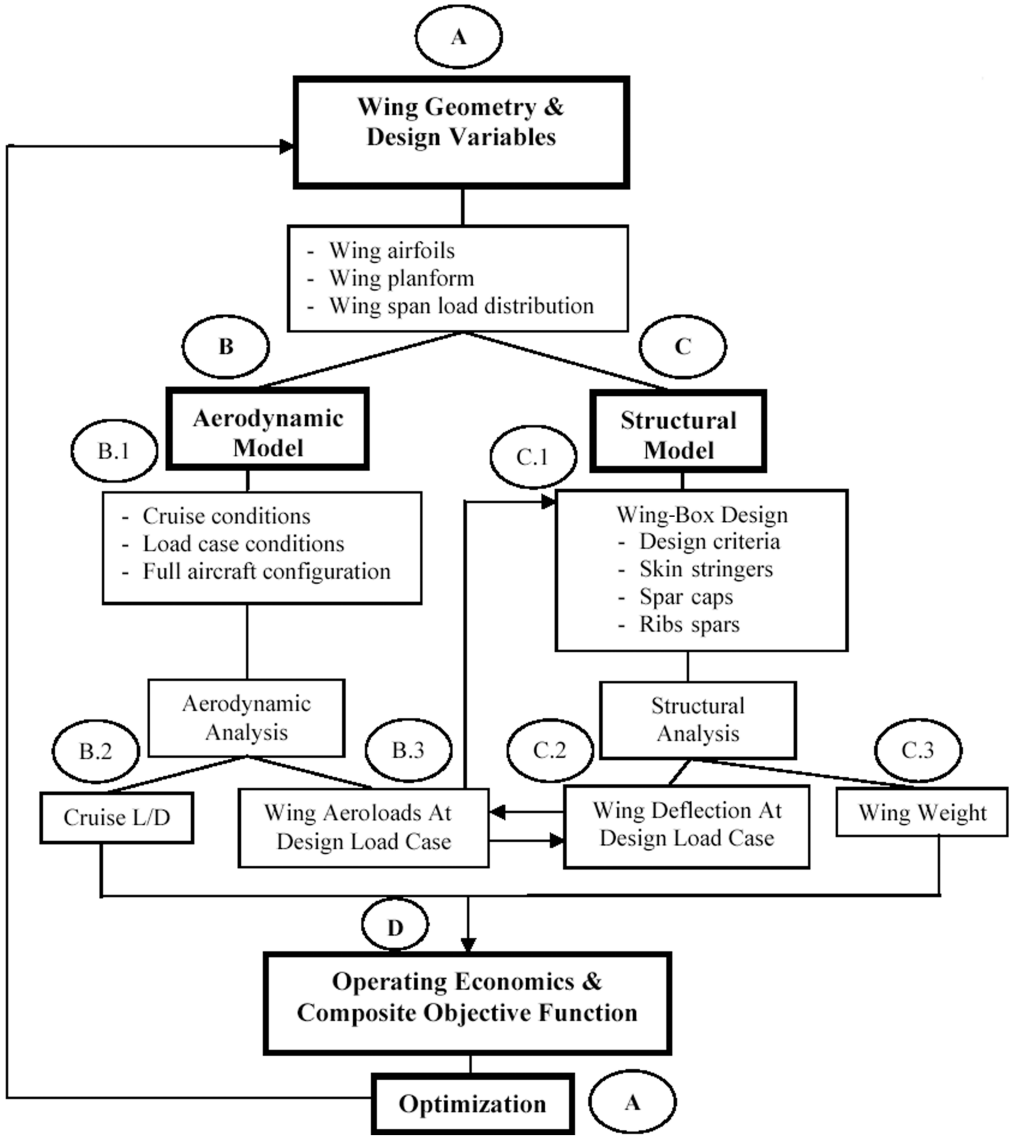

Fig. 2 Flowchart of the aerostructural optimization process.

III. Aerodynamics Subspace Formulation

In the preliminary design phase of an aircraft, the design space is very large and complex, and therefore, speed of execution and automation are required to quickly evaluate a large set of potential aircraft candidates. For this reason the traditional approach in aircraft sizing has been, and still is to a large extent, the use of an aerodynamic database of empirical relations. There are major limitations with this type of approach, however. First, empirical relations are statistical in nature and cannot capture all the design variable sensitivities required to fully explore the design space. Second, the database is typically only valid for the class of aircraft configurations it is derived from, and as such, it will tend to exclude innovative concepts in the design process.

Ideally, the aerodynamic model in a conceptual or preliminary aircraft design should be capable of computing the drag of an entirely new configuration. This model must also be able to provide trimmed aircraft polars for not only one aircraft, but typically for a family of aircraft derived from the baseline currently being considered. It is also often the case that a new aircraft concept has only generic definitions of some of its component geometry, and is a modular construct based on various wing dimensions, cabin layouts, one or more engine candidates, and various control surface configurations.

As noted earlier, the approach adopted here is to separate the design process into two stages, namely, a conceptual-preliminary stage, and a detailed design stage. In the conceptual-preliminary stage, what is required is an optimization strategy capable of finding the global minimum in a complex design space with multiple constraints. In this context, a low-cost analysis method is needed to compute large numbers of direct function call evaluations.

The CFD code that is currently used for this purpose at Bombardier is called KTRAN [31–33]. KTRAN solves a modified TSD equation using Cartesian grid embedding techniques, coupled to boundary layer calculations on the aircraft lifting surfaces. Although the TSD approach is a 30-year old technology in the field of CFD, in the world of conceptual-preliminary aircraft design, it provides a significant advantage over a purely empirical database.

The KTRAN program provides reliable predictions of wing pressure distributions, drag, and aerodynamic loads at aircraft design conditions, that is, at conditions with relatively weak shock waves and attached flow. It can be used to model full aircraft configurations in a modular fashion, including fuselage-mounted or wing-mounted nacelles, wing-tip winglets, and vertical and horizontal tail components that can be either fuselage mounted or in a T-tail configuration.

The reliability of the drag prediction in KTRAN stems from the fact that it employs a mix of empirical and computational drag prediction methods. Empirical relations are used to compute the drag of all the nonlifting components of the aircraft (fuselage, nacelles,

pylons, vertical tail, fairings, and all forms of excrescences), and computational methods are used to compute the drag of all the lifting surfaces (wing, winglets, and horizontal tail). The empirical formulas used for the nonlifting components are implementations of well-known methods, for example, Hoerner [34], modified for Bombardier applications and validated in various wind-tunnel tests. The empirical formulas are quite accurate in subsonic conditions, but progressively less so in the higher transonic region, where compressibility effects or wave drag may begin to appear on the nonlifting components. However, for a well-designed aircraft, these effects are quite small in design cruise conditions. Furthermore, because these formulas are not used to compute the wing drag during the optimization, any small error in the drag of the nonlifting components will not significantly bias the wing optimization.

For the drag of the lifting surfaces, the computational methods provide a breakdown of the drag into its three basic components, that is, viscous drag, lift-induced drag, and wave drag. The compressible Squire–Young formula, integrated over the wing span, is used to compute the viscous drag from the boundary layer computations. Lock's method [35] is used to compute the drag due to shock waves, and a nonplanar vortex sheet method is employed to compute lift-induced drag of the wing, winglet, and tail surfaces. The trim drag of the aircraft is calculated using Munk's theorem [36], which has been implemented in KTRAN.

Figure 3 provides a comparison of a KTRAN prediction with wind-tunnel measurements of the wing pressure distribution for the Bombardier Challenger aircraft, at $M = 0.82$, $C_L = 0.64$. This condition is close to buffet onset for this aircraft. In Fig. 4, the drag prediction capability of the code is illustrated with a comparison of the Challenger 300 aircraft trimmed drag polars measured in flight test. Similar correlations have also been obtained for other Bombardier aircraft. The accuracy of the drag computed by the code is usually within 2–3% of flight test measurements in design cruise conditions.

The coupling of a low-fidelity analysis code to an efficient optimizer is not a straightforward matter. This is because a good optimizer will always try to "abuse" any weakness in the analysis code. In the case of KTRAN, checks were implemented in the program to limit the adverse pressure gradient in the aft portion of the wing upper surface, to preclude airfoil designs with trailing edge separation. The specific gradient limit chosen was based partially on experience drawn from previous designs, and partially on airfoil optimizations performed with high-fidelity (Navier–Stokes) codes.

The viability of the KTRAN code in an aggressive optimization environment was evaluated by comparing the performance of two-dimensional airfoils optimized with KTRAN to airfoils optimized with Navier–Stokes codes. On average, it was found that the sectional lift-to-drag ratios of airfoils optimized with KTRAN, and

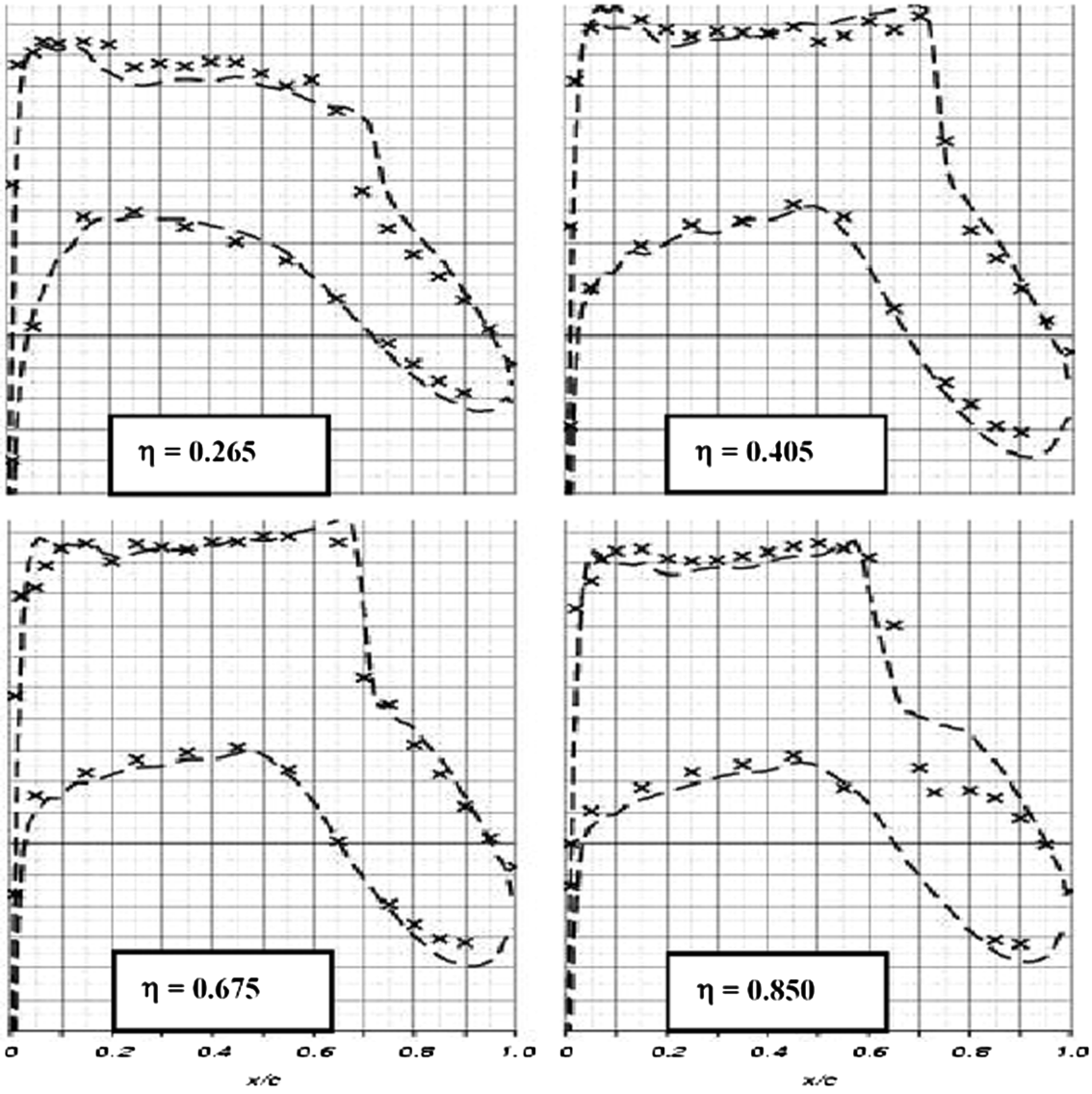

Fig. 3 KTRAN wing pressure distribution versus wind tunnel for Challenger aircraft at $M = 0.82$, $C_L = 0.64$.

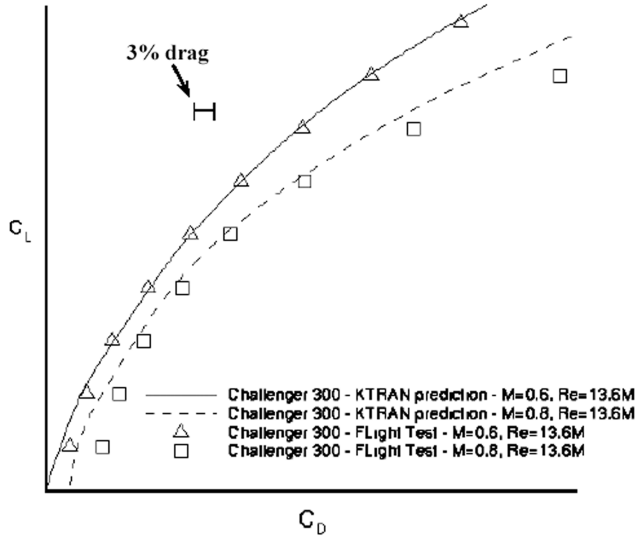

Fig. 4 KTRAN drag prediction versus flight test for the Challenger 300 aircraft.

later evaluated with a Navier–Stokes code, were only 1–2% lower than airfoils optimized directly with the Navier–Stokes code (for equivalent two-dimensional flow conditions in the range of $M = 0.70$–0.75,[¶] and $C_L = 0.70$–0.80). This important result, along with the correlations presented in Figs. 3 and 4, illustrate the viability of KTRAN and its relevance in an aircraft preliminary design environment. Furthermore, the computer time required to obtain a KTRAN solution on a trimmed, full aircraft configuration is only 90 s on a single processor of an IBM P5-575 machine equipped with Power 5 processors.

IV. Structural Subspace Formulation

Several structural design modules were developed to size various essential components of the wing box. These design modules were incorporated in a code called TWSAP [27–29], which is used to define a conceptual layout of the wing structure. TWSAP generates a beam finite element model representation of the wing structure to calculate the wing structural properties.

The design process begins by distributing the ribs within the wing box and designing the sections at the ribs' locations one after the other along the wing span. The wing external geometry is assumed to be known at the beginning of the design process as well as the location of the front and rear spars for each section. Figure 5 shows two conceptual rib and spar layouts generated by the TWSAP program. The program is capable of generating streamwise, fanned, and normal-to-rear spar ribs.

At each rib location, the structural layout is idealized by the skin, stringers, spars, and spar caps. The skins, stringers, and caps are sized based on structural failure modes and design loads (load intensity curves). The process of generating the conceptual spanwise design loads, which are used in the sizing process of the wing-box skin-stringer panels and spar-cap assemblies, was developed into a design module. In TWSAP, the spars are considered as diagonal tension webs [37].

A methodology was developed for the conceptual design of stringer-stiffened compression panels [29]. The design method includes local (based on plate theory) and general (based on Euler–Engesser or Johnson–Euler column stress) failure modes common to aerospace compression structures. It also takes into account the panel beam-column analysis. The present skin-stringer design module is capable of sizing panels with different types of stringers such as the so-called "J" and "Z" types.

[¶]This two-dimensional Mach number range is equivalent to $M = 0.77$–0.83 for a three-dimensional wing with 25 deg quarter-chord sweep.

The design loads are extracted from the aerodynamic and inertial loads. The load intensity curves depend on the height and width of the box at the rib location, which in turn depend on the aerodynamic profile (airfoil shape) at that location.

Once the structural details (geometry of the box, skin thickness, stringer area, etc.) at each rib location have been sized, the thin-walled cross-sectional properties of the box are then computed. The structure of a wing box is complex in nature. It contains many elements that make the structural analysis process a very long and difficult one. The present method for structural analysis depends on a numerical procedure that is applied to determine the torsional and flexural properties of multicellular cross sections, which are used frequently in modern wing structures [28]. The TWSAP program uses thin-walled, single cell sections to represent the wing box. Each wing-box section is modeled with a set of skin-stringer panels, front and rear spars, and upper and lower spar caps, as shown in Fig. 6.

Upon completion of the numerical calculations of the stiffness properties for all the box sections at the rib locations (along the wing span), a finite element beam model of the conceptual structure is generated. This model can be used to predict the deformation of a wing that has yet to go through detailed design.

The difficulty in conceptual-preliminary design is to develop aeroelastic models that are sufficiently simple to be called thousands of times during optimization, but are sophisticated enough to accurately predict wing deformations. Simplified beam finite element models of aircraft wing structures, also known as stick models, are often used for aerodynamics-structures interaction. Such models can be used for both static and dynamic aeroelastic analyses.

The stick model of a wing structure is a series of tapered or uniform beam or bar elements, as shown in Fig. 7. The TWSAP program automatically generates the stick finite element model of the conceptually designed wing.

V. Aerostructural Coupling and Validation

The objective of coupling aerodynamic and structural models is to compute the flow over flexible wings. The aerodynamic forces computed by aerodynamic analysis codes are integrated to obtain the shear forces. The shear forces are then applied to the stick model to obtain the deformed condition of the wing. In the first iteration, the aerodynamic loads are calculated for the undeformed wing (initial geometry, usually the jig geometry).

The initial values of the wing vertical deflection and twist are obtained from the NASTRAN [30] solution. NASTRAN results are then coupled to the CFD analysis by modifying the wing twist and bending in the CFD model. A new set of loads is then obtained. The new set of shear forces is then given to NASTRAN to obtain a more accurate set of wing deflection and twist. This iterative procedure is repeated until the coupled solution converges.

Convergence is reached when the difference between the twist of a previous iterative step and the current step is smaller than a user-specified criterion. Convergence represents the quasi-static aeroelastic equilibrium state of a wing. Figure 8 shows the quasi-static aeroelastic equilibrium state of a test wing obtained using the present method.

To validate TWSAP, the program was used to design a conceptual wing structure for the Bombardier Global Express aircraft wing, given only the wing external lines and a representative (2.5 g maneuver) set of design loads. Figure 9 shows the comparison of the spanwise stiffness distribution of the actual and conceptual wings, showing an excellent agreement. This result illustrates how a very good estimate of the wing stiffness can be obtained with a conceptual or preliminary design tool.

VI. Quasi-Analytical Weight Prediction Method

As noted earlier, the wing structural weight, which includes the high-lift devices, can be estimated from semi-empirical relationships (GASP [26]). Applications of this method originate from work conducted by Burt [38] and Shanley [39] who examined ways in which the prediction of wing weight can be based on elementary

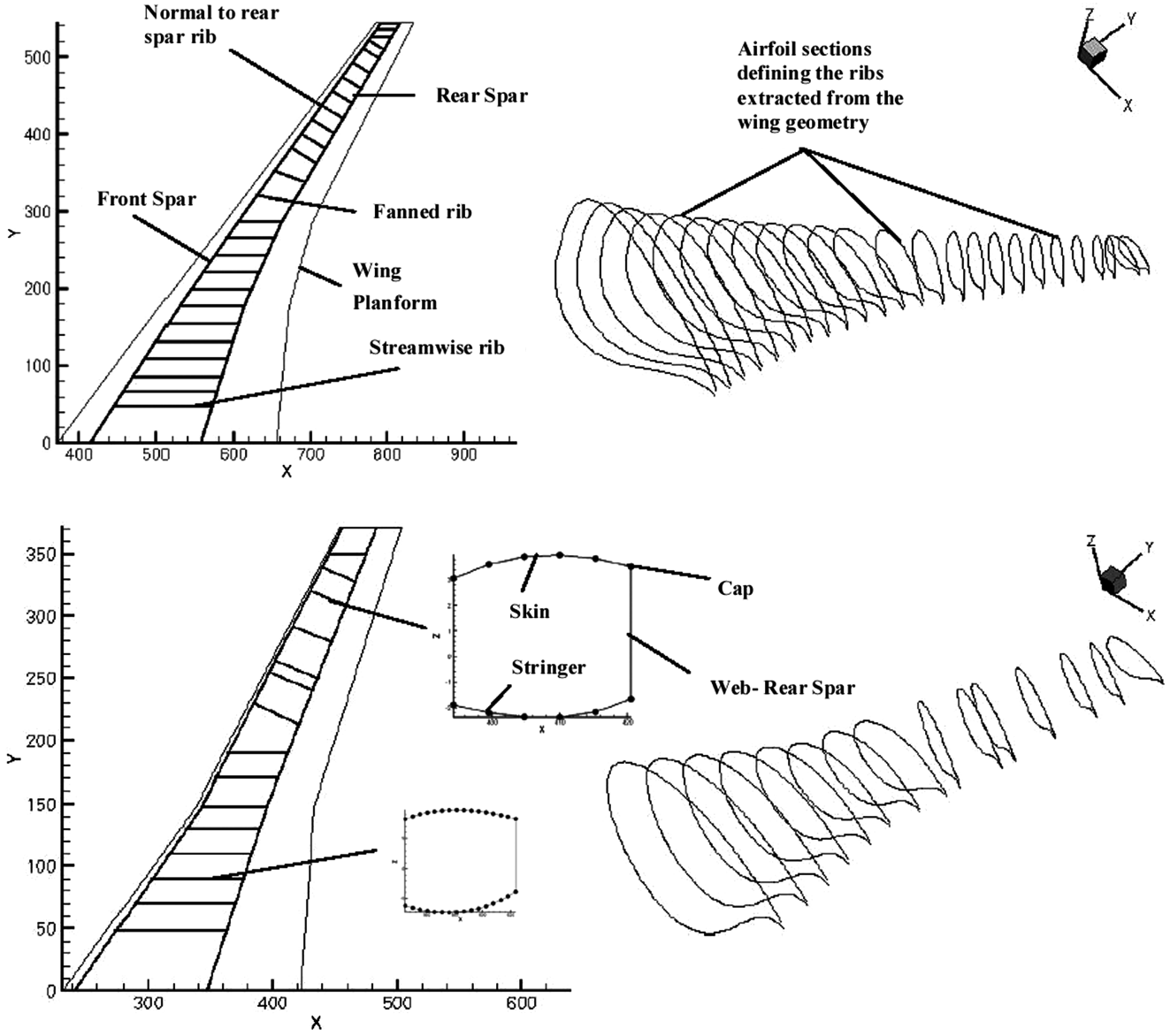

Fig. 5 Two conceptual rib and spar layouts generated by TWSAP.

strength and stiffness considerations with adjustments incorporated according to experimental and statistical data. GASP is applicable to a wide range of subsonic aircraft.

Although GASP can be used to provide a reasonably good estimate of the wing weight, in the present method it is used only to provide an initial estimate. GASP is not used in the optimization process because it lacks the capability of capturing the sensitivities of the wing weight to detailed changes in wing sectional profiles and to changes in the wing span load distribution, which are design variables in the present optimization method.

A more detailed estimate of the weight sensitivities is obtained by using the structural model of the wing box designed by TWSAP [27–29]. In this way, wing weight changes due to spanwise variations in design loads and wing-box properties are captured. After predicting the wing weight component related to the skin-stringer panels and the front and rear spars, the ribs' weight is estimated next based on the well-known Farrar method [40]. The weights of the wing components outside of the wing box, including the leading and trailing edge control surfaces, are predicted in isolation using the empirical estimates of GASP.

In addition, to account for the weight of miscellaneous items such as fasteners, cutouts, splices and joints, fuselage attachment, fuel containment, and all other unique features of the aircraft wing box under analysis, a series of statistically based increments are applied. This task has been accomplished by using the component weight factors method developed by Wakayama and Kroo [15], which provide appropriate regression factors (for each wing-box structural component such as the panels and ribs) applicable to commercial and executive category transport aircraft. The present method has been validated by comparison with the absolute wing weight of Bombardier's Challenger and Global Express aircraft, for which the method's prediction errors were within 6 and 3%, respectively.

VII. Operating Economics and Composite Objective Function

A series of prediction algorithms originally intended for the predesign stage of transport aircraft design were incorporated into the ASO environment. The prediction methods are a hybrid of statistical correlations of design variables and macroobjective functions with fractional change analytical constructs [25]. The analytical component of the fractional change method operates with the underlying premise that the designer/analyst begins with a seed condition or aircraft. Once a basic list of fundamental design variables and functions are known, prediction of variations away from the seed aircraft can then be conducted. Validation work [25]

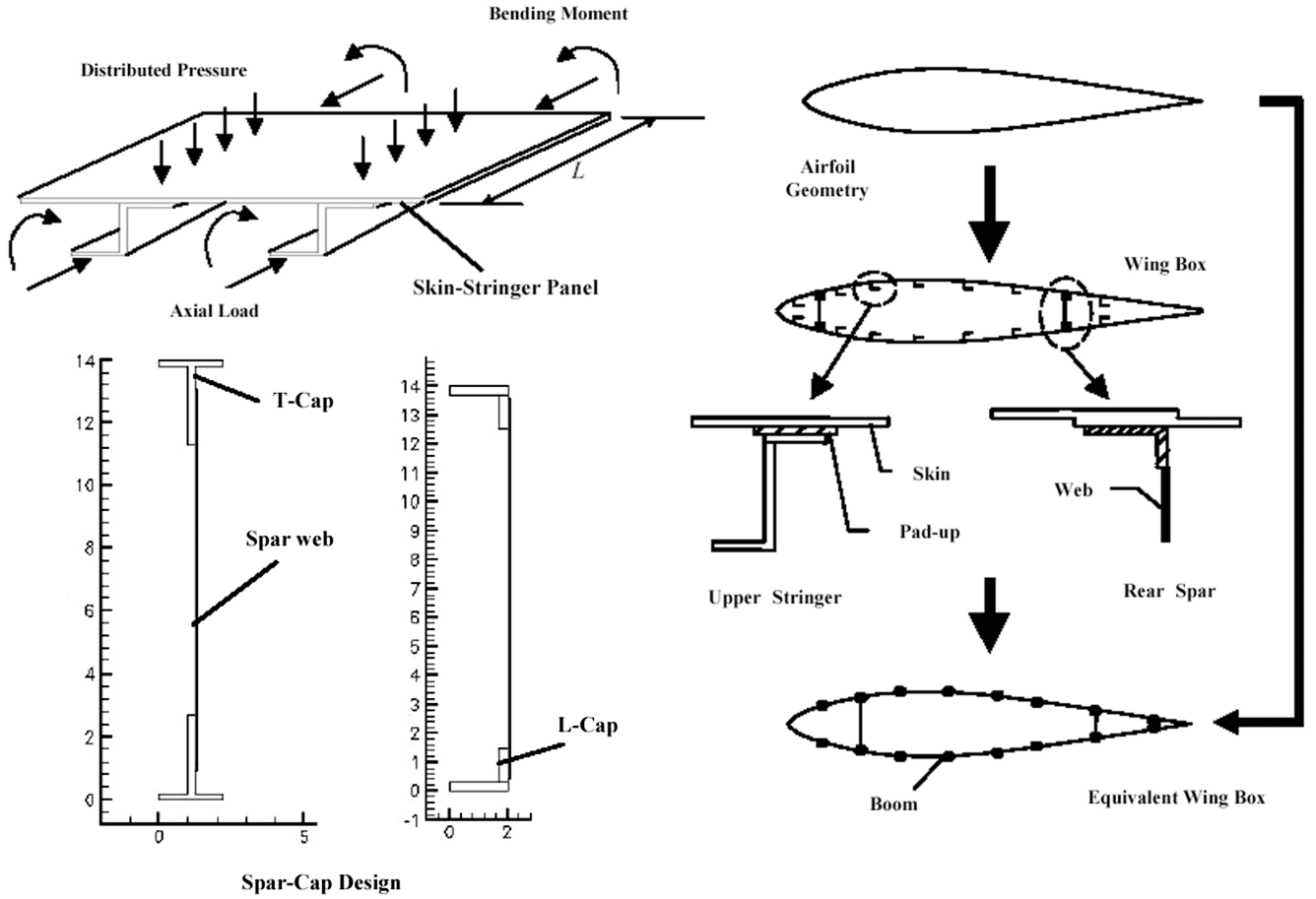

Fig. 6 Typical stringer-stiffened compression wing panel and spar-cap design (left) and equivalent wing box extracted from the actual structure (right).

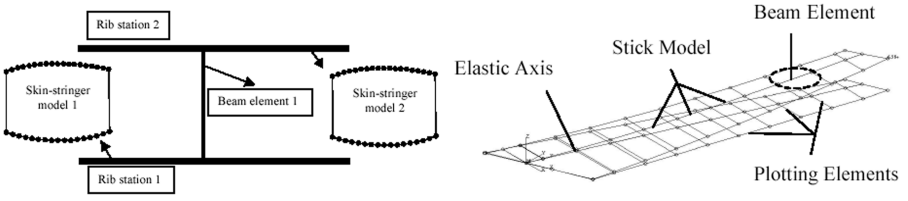

Fig. 7 Typical beam finite element model.

a) The *undeformed* condition

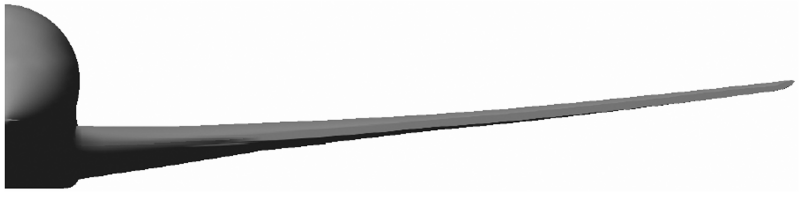

b) The *deformed* condition

Fig. 8 The quasitatic aeroelastic equilibrium state of a test wing.

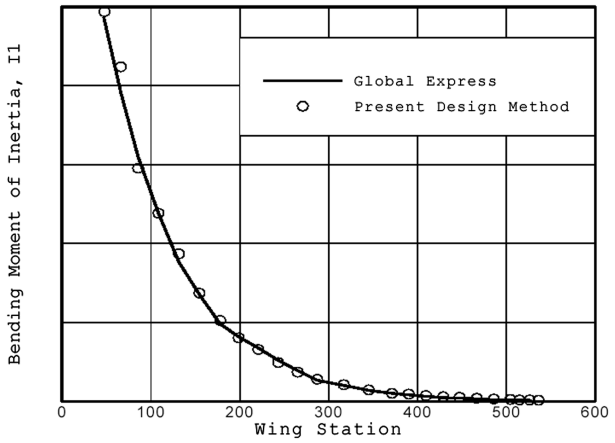

Fig. 9 Comparison between the bending moment of inertia of the Global Express ultralong range business jet and the conceptually designed one.

has established the applicability of these prediction algorithms for personal/microturbofan aircraft, business aircraft from very light to ultralong range categories to commercial aircraft from commuters to narrow-body transports of around 100 passengers. The suite of fractional change algorithms covers atmospheric and general properties as well as five subspaces: geometric characteristics, weights, low-speed and high-speed aerodynamics, engine performance, and operational performance.

The fractional change methodology used in the present ASO program focuses on the prediction of cash operating cost (COC) and en route performance attributes. Although normally COC is not considered to be an important objective for business aircraft design optimization, the COC model for North American operations was scrutinized for eligibility and finally designated as the objective function for this exercise. As will be shown in the review to follow, the final model for COC was reasoned as being directly proportional to the fractional change in mission fuel. Thus, the ASO problem statement was reduced to that of minimizing the mission fuel mass, which in turn represents a major contributory component in the COC model.

A. Concept of Fractional Change

As stated earlier, the analytical component of the fractional change method assumes that the designer/analyst begins with a seed condition/aircraft. By considering an increment in variable x as dx or Δx, a fractional change to a new value x_1, small or otherwise, in a seed parameter x_0 is defined as

$$\triangleleft x = \frac{\Delta x}{x_0} = \frac{x_1 - x_0}{x_0} \tag{1}$$

This has the property of quantifying a relationship between the initial condition and any subsequent variations, which can be used to derive solutions with less effort. A special set of rules of operation must be defined to execute a treatment of functional transformations. For purposes of this task, a multivariable association (with accompanying partial fraction expressions) and product and/or quotient of multiple independent variables expressed in exponent form are transformed to be

$$z = \pm x \pm y \Rightarrow \triangleleft z = \chi_x \triangleleft x + \chi_y \triangleleft y, \quad \text{where } \chi_x = \frac{\pm x_0}{\pm x_0 \pm y_0}$$

$$\chi_y = \frac{\pm y_0}{\pm x_0 \pm y_0} \tag{2a}$$

$$z = x^a y^{-b} \Rightarrow \triangleleft z = \frac{(1 + \triangleleft x)^a}{(1 + \triangleleft y)^b} - 1 \tag{2b}$$

where z is an arbitrary dependent parameter, and x and y are arbitrary independent parameters or design variables.

B. Operating Economics

To establish COC as a primary metric for business aircraft optimization, it is worthwhile examining the market in which the aircraft is to operate. Today there are five distinct ways business aircraft can be owned or chartered as follows:

1) traditional ownership—outright ownership and complete responsibility for operation;

2) new and used fractional ownership—allotment of time based on a given fractional ownership of a new or used business jet;

3) branded charter—privately owned fleet of similarly outfitted business jets offering chartered service;

4) "by-the-seat" charter—chartered seats sold in scope similar to commercial operators;

5) business airline charter—regularly scheduled flights using business jets between city pairs deemed profitable.

The traditional business aircraft ownership is the most dependable means of travel, but comes at an appreciable expense. As a result, the charter services and fractional ownership have demonstrated to be schemes attracting the majority of upper echelon commercial aviation customers as well as enticing clientele who would normally not purchase business jets to consider fractional ownership. In view of this market dynamic, reduction in operating economics becomes one key aspect of the marketing requirements and objectives and, therefore, should be considered as a primary objective function for any ASO exercise.

Ownership is dictated by commercial concerns (aircraft's next available price the market is willing to absorb), thus, the DOC model was dropped in favor of a COC one in an attempt to avoid distortions that would occur when assessing economic efficiency due to uncertainty in the aircraft's next available price.

The COC model for North American operations used in this formulation comprises crew, block fuel, maintenance, and landing fee cost constituents [41]. Written in algebraic form, the COC model is

$$\text{COC} = C_{\text{crew}} t + C_{\text{fuel}} W_{\text{fuel}} + C_{\text{mnt}}(t - t_{\text{man}}) + C_{\text{mnt cyc}} + C_{\text{mnt eng}} f(\delta) + C_{\text{fees}} \text{MLW} \tag{3}$$

The mission block time is given by t and block fuel by W_{fuel}. C_{crew} is the hourly cost of the flight (and cabin) crew. C_{fuel} is the price of fuel in cost units (CU) per unit weight. C_{mnt} is the time dependent maintenance cost in CU per flight hour, with flight hours expressed as a difference between block time and t_{man}, the fixed maneuver allowance. $C_{\text{mnt cyc}}$ is the cyclic airframe maintenance cost. $C_{\text{mnt eng}}$ is the cyclic maintenance component that is assumed to have a functional dependency on the engine derate level, $f(\delta)$. C_{fees} is the landing fee charge in CU per unit weight based on the maximum landing weight (MLW). As exemplified by Torenbeek [42], an initial prediction of MLW can be generically based on the design range (at design payload), maximum zero-fuel weight (MZFW) and maximum takeoff weight (MTOW) of an aircraft candidate. For a given business aircraft design intent it can be assumed that MZFW is essentially invariant and the design range (and design payload) is constant, thus leading to a functional association between MLW and MTOW only. After conducting a fractional change transformation of Eq. (3), the model becomes

$$\triangleleft\text{COC} = (\chi_{\text{crew}} + \chi_{\text{mnt}}) \triangleleft t + \chi_{\text{fuel}} \triangleleft W_{\text{fuel}} + \chi_{\text{mnt eng}} \triangleleft f(\delta) + \chi_{\text{fees}} \upsilon_{\text{MTOW}} \triangleleft \text{MTOW} \tag{4}$$

with υ_{MTOW} representing a MTOW partial fraction required to establish a functional association between $\triangleleft$MLW and $\triangleleft$MTOW.

Quite often, it is more convenient to gauge the variation of flight fuel (W_{flt}) instead of block fuel ($W_{\text{fuel}} = W_{\text{flt}} + W_{\text{man}}$) because one can forego the sometimes unnecessary complication of considering the block maneuvering allowance (W_{man}). Although this inference is not appropriate for short-haul operations, it is an acceptable

simplification for long-range missions (like those conducted by business aircraft) since W_{flt} is at least 2 orders of magnitude larger than W_{man}. Assuming either no change in block maneuvering allowance, or, that the cascaded result is small, the approximate expression, $\triangleleft W_{\text{flt}} \cong \triangleleft W_{\text{fuel}}$, can be considered valid.

For purposes of this particular ASO exercise, assuming small changes in flight time (same speed schedule), neglecting adjustments in maintenance cost due to changes in engine derate, and since the landing fees remain fixed because for the present application the design weights are kept constant, the final simplified fractional change model for COC in North America becomes

$$\triangleleft \text{COC} \cong \chi_{\text{flt}} \triangleleft W_{\text{flt}} \tag{5}$$

The goal for any ASO or MDO exercise should be to minimize the result generated by Eq. (5).

C. Integrated Range Model

A complete National Business Aircraft Association (NBAA) instrument flight rules (IFR) mission flight profile trajectory as depicted in Fig. 10 consists of three consecutive segments: climb, cruise, and descent. Each segment is subject to transversality conditions that depend on the endpoint constraints of state variables, thus the entire flight must be analyzed as a global problem wherein the links between all the phases are considered concurrently. A sector mission is the operation of an aircraft from the start of en route climb to the end of approach. Unique and constant values of calibrated airspeed (CAS) [(or indicated airspeed (IAS)] and M, for corresponding throttle setting, are indicative of each phase with strategic switches in CAS/throttle effected during the flight. Flight time and flight fuel also include allowances required for takeoff, initial climb, and approach. The block time and block fuel includes additional allowances for startup and taxi-out. Each sector mission analysis will have with it an associated reserve fuel that is carried to destination.

Derivation of a new integrated range model (IRM) begins with the Breguet equation for range (R). In differential form the Breguet equation accounts for the change in aircraft instantaneous gross weight, or, all-up weight (AUW; W) based on an instantaneous specific air range. One variation of the differential equation for range is to express it as a function of fuel calorific value (H), the overall power plant efficiency ($\eta_e \simeq$ combustion efficiency$\times$ thermal efficiency $\times$ propulsive efficiency) and the vehicular L/D

$$dR = \frac{H}{g}\eta_e (L/D)\frac{dW_{\text{fuel}}}{W} \tag{6}$$

Equation (6) quotes only increments in range for an instantaneous condition. The actual aim is to seek an integrated range result wherein the product of η_e (L/D) continually varies for the entire mission. One method is to assume an arbitrary reference point such as the initial cruise altitude (ICA) is related to the TOGW, where $W = k_{\text{clb}}\text{TOGW}$, $k_{\text{clb}} < 1$, and incorporate a profile correction (Θ_{prf}) that captures step cruising as well as the dynamic η_e (L/D) effect. The profile correction coefficient value will be unique depending on the relationship between AUW at the ICA and the AUW at the end of mission. In view of this association and because account is made for AUW at the initial cruise in Eq. (6), it is reasonable to conclude that proportionality will exist between Θ_{prf} and zero-fuel weight, that is, ZFW = basic operating weight (BOW) plus payload, and a suitable relationship has been established to be an exponential one, that is, $\Theta_{\text{prf}} = (1 + \triangleleft\text{ZFW})^{\varepsilon}$. To permit an even wider scope of functional sensitivity with sufficient accuracy, an extension to the profile correction [25] would also include an account of the variations due to a change in the useful load as the payload remains fixed, that is, fuel burn off and hence TOGW varies. This relationship was also found to be suitably represented by an exponential one with $\Theta_{\text{prf}} = (1 + \triangleleft\varsigma_{\text{flt}})^{\alpha}$, where $\triangleleft\varsigma_{\text{flt}}$ represents the flight fuel fraction or $\triangleleft\varsigma_{\text{flt}} = (1 + \triangleleft W_{\text{flt}})/(1 + \triangleleft\text{TOGW}) - 1$.

Upon introduction of an extended Θ_{prf} definition into the integration of Eq. (6), the method to quantify fractional change in range becomes

$$\triangleleft R = \frac{(1 + \triangleleft\eta_e)[1 + \triangleleft(L/D)](1 + \triangleleft\varsigma_{\text{flt}})^{\alpha}}{(1 + \triangleleft\text{ZFW})^{\varepsilon}} - 1 \tag{7}$$

Typical intervals of values for transport aircraft with respect to mission dependent regression coefficients are $\alpha = 1.36$ to 3.08 and $\varepsilon = -1.14$ to -0.36.

The η_e parameter varies with both throttle setting and cruise speed; in general, speed has a greater effect on η_e than throttle setting, and η_e improves with increasing speed. Assuming a linear relationship between corrected thrust specific fuel consumption (TSFC) and

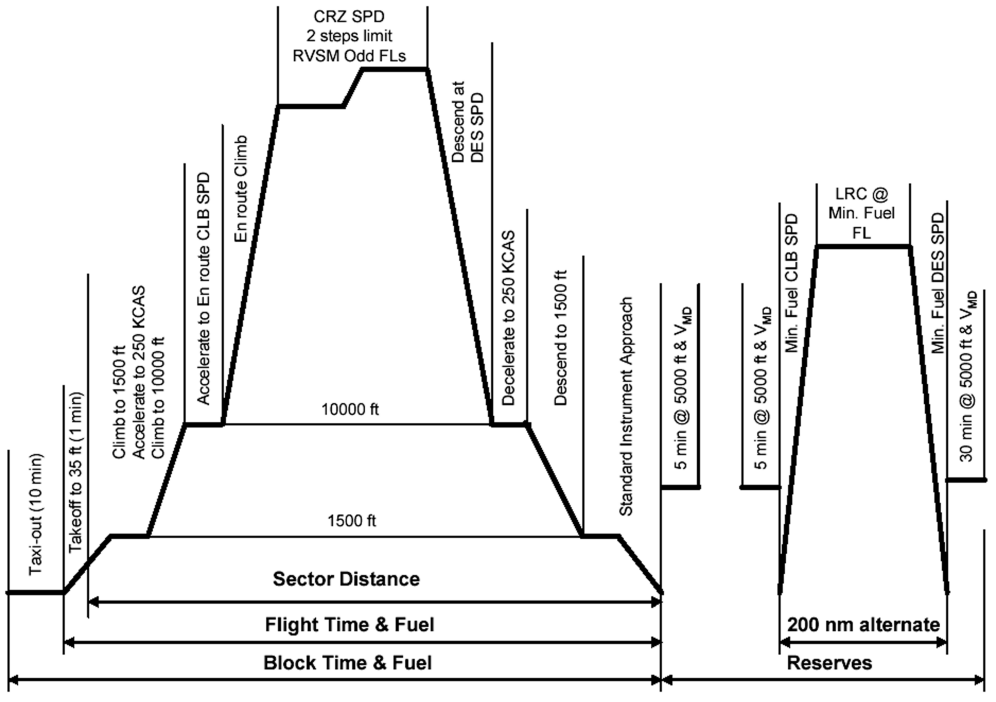

Fig. 10 Elucidation of the NBAA IFR flight profile. CLB = climb; CRZ = cruise; DES = descent; FL = flight level; LRC = long range cruise; RVSM = reduced vertical separation minima.

speed [43], and neglecting the effect of throttle, the fractional change in η_e becomes

$$\triangleleft\eta_e = \frac{(1+\triangleleft M)(1+\tau_M)}{1+\tau_M(1+\triangleleft M)} - 1 \tag{8}$$

with $\tau_M = k_M M_0$, where the parameter k_M is derived empirically and is specific to the engine being modeled, and M_0 is the reference or seed Mach number.

The flight fuel for a complete mission profile is defined as the release fuel (total fuel) less the summation of quantities devoted to block maneuvering, hold, and diversion. Adhering to this fuel balance relationship, the fractional change in ς_{flt} is

$$\triangleleft\varsigma_{\text{flt}} = \frac{\triangleleft\varsigma_{\text{rfl}} - \chi_{\text{man}}\triangleleft\varsigma_{\text{man}} - \chi_{\text{hld}}\triangleleft\varsigma_{\text{hld}} - \chi_{\text{div}}\triangleleft\varsigma_{\text{div}}}{1 - \chi_{\text{man}} - \chi_{\text{hld}} - \chi_{\text{div}}} \tag{9}$$

where the partial fractions are referenced to the seed as

$$\chi_{\text{man}} = \frac{\varsigma_{\text{man0}}}{\varsigma_{\text{rfl0}}} \tag{10a}$$

$$\chi_{\text{hld}} = \frac{\varsigma_{\text{hld0}}}{\varsigma_{\text{rfl0}}} \tag{10b}$$

$$\chi_{\text{div}} = \frac{\varsigma_{\text{div0}}}{\varsigma_{\text{rfl0}}} \tag{10c}$$

and where the following are further defined as fuel fractions:

$$\varsigma_{\text{rfl}} = \frac{W_{\text{rfl}}}{\text{TOGW}} \tag{11a}$$

$$\varsigma_{\text{man}} = \frac{W_{\text{man}}}{\text{TOGW}} \tag{11b}$$

$$\varsigma_{\text{hld}} = \frac{W_{\text{hld}}}{\text{TOGW}} \tag{11c}$$

$$\varsigma_{\text{div}} = \frac{W_{\text{div}}}{\text{TOGW}} \tag{11d}$$

for release, block maneuvering, holding, and diversion fuels, respectively.

Using Eq. (7) as a basis, neglecting the profile correction coefficient and assuming an invariant η_e, the holding fuel fractional change operation becomes

$$\triangleleft\varsigma_{\text{hld}} \cong \frac{1}{1+\triangleleft(L/D)_{\text{hld}}} - 1 \tag{12}$$

For a fixed diversion distance, Eq. (7) is rearranged such that the fuel fraction becomes the subject; assuming an invariant η_e, the expression for the diversion fuel fractional change is

$$\triangleleft\varsigma_{\text{div}} \cong \frac{(1+\triangleleft\text{ZFW})^{\lambda}}{1+\triangleleft(L/D)_{\text{div}}} - 1 \tag{13}$$

Values for the aircraft and mission dependent regression coefficient λ can vary between -0.34 and $+0.71$.

It must be noted that in both Eqs. (12) and (13), the computations for L/D should be referenced against ZFW, and the corresponding typical altitudes and speeds for these flight phases.

To exemplify the applicability of the derived formulation of the integrated range, a validation was conducted by coalescing out the α and ε regression coefficients generated through batch calculations of the Challenger CL-604 using Bombardier Aerospace's in-house developed Canadair Aircraft Synthesis Program (CASPR) and then comparing the regression coefficients' robustness to that of the original batch calculations. The batch calculations comprised executing numerically integrated mission performance for concurrent intervals of TOGW = [0.87 Opt MTOW, Opt MTOW] where Opt MTOW represents an optional MTOW, Payload = [0, Max Payload], and, $M = [0.74, 0.80]$. Figure 11 depicts the performance of Eq. (7) using the seed values and derived correlation coefficients.

As can be seen in Fig. 11, the IRM produces a satisfactory result with the majority of dataset points falling within a relative range of approximately $-0.5 \leq E \leq +0.5\%$ and absolute $-15 \leq E \leq +20$ nm error bandwidth. Outliers from this interval of error are considered to be extreme cases, that is, maximum payload or ferry flight; notwithstanding this circumstance, the error does not exceed approximately $\pm 1.0\%$, or, $+30$ nm and -40 nm.

D. Composite Objective Function

Based on the foregoing analysis, an algebraic expression that equates the aerodynamics and structures tradeoff explicitly can be derived as follows.

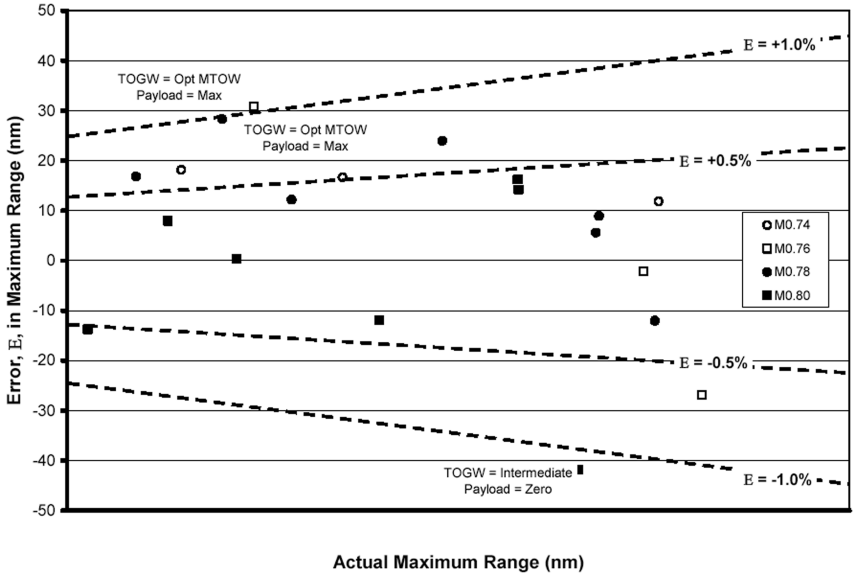

Fig. 11 Plot of predicted maximum range and associated error for the Challenger CL-604 using the integrated range model.

Taking Eq. (7), rearranging it to isolate $\triangleleft\varsigma_{\text{flt}}$, and introducing a substitution parameter f, we obtain

$$\triangleleft\varsigma_{\text{flt}} = \left\{\frac{(1+\triangleleft R)(1+\triangleleft\text{ZFW})^{\varepsilon}}{(1+\triangleleft\eta_e)[1+\triangleleft(L/D)]}\right\}^{1/\alpha} - 1 = f - 1 \tag{14}$$

Recalling that the fractional change in flight fuel fraction can also be expressed in the following form:

$$\triangleleft\varsigma_{\text{flt}} = \frac{1+\triangleleft W_{\text{flt}}}{1+\triangleleft\text{TOGW}} - 1 \tag{15}$$

By equating Eqs. (14) and (15), it can be shown that a new prediction of the flight fuel is given by

$$W_{\text{flt1}} = \frac{f\varsigma_{\text{flt0}}}{1-f\varsigma_{\text{flt0}}}(\Delta W_{\text{STR}} + \text{ZFW}_0 + W_{\text{man1}} + W_{\text{res1}}) \tag{16}$$

where ΔW_{STR} is the change in structural empty weight from the reference manufacturer's weight empty (MWE_0) for a given iteration in the active ASO/MDO scheme, and W_{res} is the combined hold and alternate reserve fuel quantity.

One difficulty with the complete IRM of Eq. (16) is that the analysis requires computing the L/D at three different flow conditions (initial cruise, initial holding, and initial diversion). This causes an undesirable increase in computation time due to the fact the CFD code needs to be run 3 times—particularly if one considers that the total reserve fuel quantity for a long-range business aircraft mission is an order of magnitude smaller compared to the flight fuel. In an effort to reduce the number of CFD computations, constituent expressions within Eq. (16) have been reworked with the aim of introducing simplifications while retaining consistency of the result for optimization purposes.

In an effort to recognize changes to the aerodynamic efficiency of the airframe for the complete integrated flight and contingencies, a basic account of this can be derived for holding and diversion maneuvers using Eqs. (12) and (13). Both of these relations indicate that a fractional change in the total reserve fuel is inversely proportional to the fractional change in locally predicted L/D; by assuming that the holding/diversion initial L/D is synonymous with the initial cruise L/D, some measure of impact to each of the contingency maneuvers can be quantified. For this purpose, a control factor (k_{aero}) is used to regulate the extent of coupling between the high-speed and intermediate-speed aerodynamic efficiencies. In addition, a sufficiently robust assumption is that the fractional change in total reserve fuel quantity is directly proportional to the fractional change in ZFW, or $\triangleleft W_{\text{res}} \cong k_{\text{res}}\triangleleft\text{ZFW}$, with k_{res} representing a constant of proportionality. Substituting a transformed (absolute value) version of this relationship into the W_{res1} component of Eq. (16), assuming no change in the block maneuvering fuel allowance, that is, $W_{\text{man1}} = W_{\text{man0}}$, and in conjunction with some algebraic factorization produces

$$W_{\text{flt1}} = \frac{f\varsigma_{\text{flt0}}}{1-f\varsigma_{\text{flt0}}}\left[\Delta W_{\text{STR}}\left(1+\frac{k_{\text{res}}W_{\text{res0}}}{\text{ZFW}_0[1+k_{\text{aero}}\triangleleft(L/D)]}\right) + \text{ZFW}_0 + W_{\text{man0}} + \frac{W_{\text{res0}}}{[1+k_{\text{aero}}\triangleleft(L/D)]}\right] \tag{17}$$

VIII. Application of ASO Methodology

The problem statement of this particular ASO task is designated as the minimization of the COC of a large business jet aircraft through the optimization of the wing planform shape and wing sectional profiles. The underlying assumption in this problem statement is that an initial sizing of the aircraft and power plant has been performed (a priori) to address the mission requirements defined for the aircraft, that is, payload, range, balanced field length, initial climb altitude capability, etc. This initial sizing defines the basic aircraft layout, MTOW, thrust-to-weight ratio, and wing loading and reference area. The objective of the ASO in this case is to minimize the COC of the aircraft for a fixed range mission, assuming a constant wing reference area and aircraft MTOW. In this optimization exercise, only the wing geometry is optimized, while the fuselage, engine, empennage, and winglet geometry and their relative positions are held fixed.

The approach adopted here effectively separates the wing sizing process from the wing shape optimization process. The motivation for this stems from the need to limit the complexity of the design space presented to the optimizer, to ensure a higher degree of success in achieving a global optimum. The premise for this approach is that once the wing planform shape and profiles have been optimized, the aircraft sizing and wing shape optimization cycles can then be repeated in an iterative loop until convergence is achieved.

A realistic aerostructural optimization of an aircraft wing must take into account all factors impacting both the aerodynamics and the structure of the wing. This includes not only high-speed aerodynamic considerations, such as lift-to-drag ratio, buffet boundary and stability and control issues, but also low-speed issues such as maximum lift coefficient and stall characteristics, etc. On the structural side, a proper design of the wing structure can only be achieved when all the critical load cases are considered.

However, in the preliminary design environment described herein, the ASO problem is simplified by taking into consideration only two representative flight conditions to design the wing: a high-speed cruise condition and a single critical load case. In the application presented here, the cruise condition is $M = 0.80$, $C_L = 0.50$, and the dimensioning load case is a 2.5 g maneuver load.

The initial aircraft configuration for this optimization exercise is shown in Fig. 12a. The complete aerodynamic representation of the aircraft, including winglets, rear-mounted engines, and a T-tail configuration is modeled in the KTRAN analysis. During the optimization, the code automatically trims the aircraft at the requested lift coefficient.

The optimization process follows the basic steps outlined in Fig. 2. The types and number of design variables, parameters, and constraints are itemized in Table 1.

In this setup, the L/D is computed by KTRAN, and the changes in wing structural weight are calculated using TWSAP. The changes in L/D and wing structural weight are fed into the integrated en route performance model to compute a composite objective function (mission fuel weight) proportional to the aircraft COC.

The optimization procedure involves four basic steps, denoted in Fig. 2 as steps A through D. In step A, the design variables and parameters defining the wing planform and sectional profiles are initialized and updated. In step B, the aerodynamic analysis of the configuration is done for both the cruise case (step B.2 in Fig. 2) and the design load case (step B.3). For the cruise case, the wing flight twist is computed to match the wing spanwise loading (the latter is initially defined as elliptic and then optimized iteratively). The aerodynamic loads calculated using KTRAN are then used to compute the wing deformation (twist and bending) using NASTRAN (step C.2), to define the wing jig twist.

For the dimensioning load case (2.5 g maneuver), the jig twist distribution is initially assumed and the loads are obtained by running KTRAN at the 2.5 g flow conditions. Once the wing is resized for stress constraints (step C.1), the wing deformations are then obtained by running NASTRAN. This process (i.e., steps B.3 and C.2) is repeated until the wing deformation has converged to within a specified tolerance (four or five iterations are usually required), in which case the quasi-static aeroelastic equilibrium condition is reached. To minimize the overall computational effort, however, the 2.5 g wing deformation is not computed at every design iteration. Instead, based on the first calculation of the 2.5 g wing loading, scale factors are computed, as a function of span position, to enable the estimation of the 2.5 g wing loading directly from the 1 g cruise loading. During the optimization process, the scale factors are updated periodically with a full flexible wing calculation to ensure an accurate representation of the loading at all times. The use of scale factors was validated and shown to provide sufficiently accurate results while greatly reducing the overall computational effort.

When the wing structure is resized (step C.1), the skin thickness, stringer pitch, stringer area, upper and lower (front and rear) spar

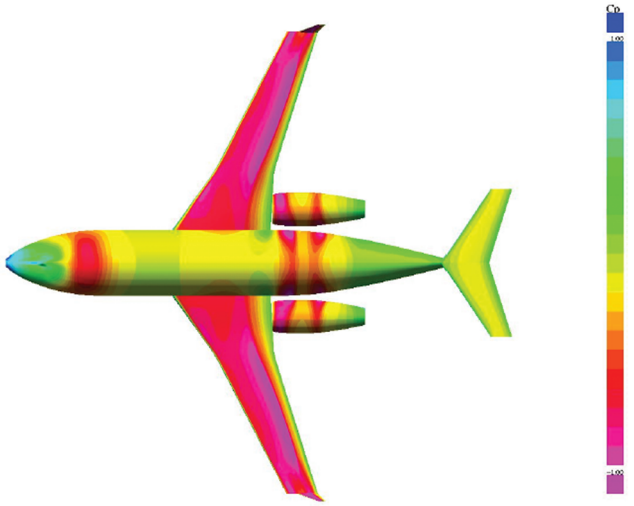

a) Aircraft configuration before aero-structural optimization

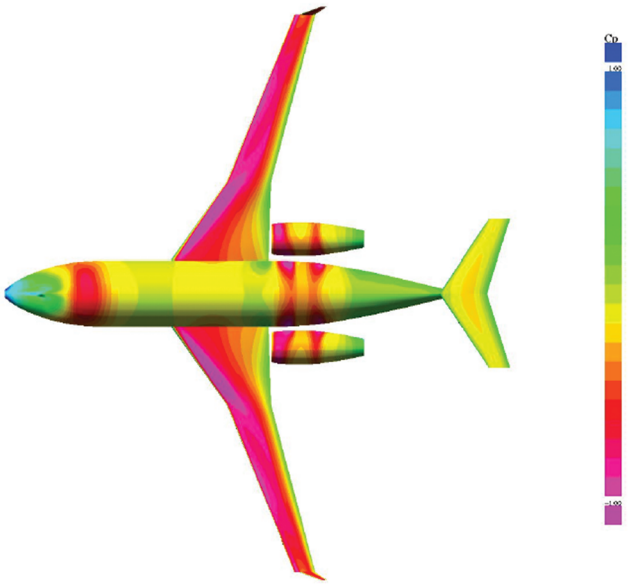

b) Aircraft configuration after aero-structural optimization

Fig. 12 a) Aircraft configuration before aerostructural optimization. b) Aircraft configuration after aerostructural optimization.

thickness and caps area are defined as structural design variables and allowed to vary along the wing span as a function of the design load intensity (bending moment over wing-box area). During the iterative process, the stringer and spar-cap geometries are fully designed, thus the thickness and area are computed (based on the methodologies described in the preceding sections). The stiffening ratio (A_{st}/A_{sk}) is set between 0.50 and 0.66 to assure that sufficient skin thickness and subsequently torque box is available to prevent wing flutter and to ensure that a sufficient stringer area is available for damage tolerance. The skin thickness is not allowed to go below 0.08 in. while the minimum load intensity is constrained to 5000 lb.in. Aluminum alloy is used for the skin-stringer panels design. The minimum and maximum strain values are set to 0.002 and 0.012 in./in., respectively. Aluminum 7075-T6 bare sheet material properties are used for the spar web while aluminum 7075-T6 extrusions are used for the spar caps and stiffeners.

Once the wing structure is resized, the wing weight (step C.3) is computed. The wing weight and the cruise L/D are then fed into step D, wherein the composite objective function is computed. The optimization process then involves repeating steps A–D until convergence is achieved.

The procedure outlined above describes the broad elements of an iterative aerostructural optimization scheme. In its early implementations, however, the procedure failed to produce designs that were anywhere near optimal. The essential reason for this failure was that the design space was simply too complex and nonlinear for any optimization algorithm to decipher in a reasonable amount of time. For a transonic aircraft, the most complex portion of the design space is the aerodynamic subspace. If an optimizer is asked to minimize simultaneously the viscous, wave, and vortex drag of a wing with several defining sections and a variable planform and span load distribution, it will tend to quickly hang in a local optimum.

The solution to this problem is to find ways to minimize the complexity of the design space in the problem setup. A way to do this is to decompose the optimization problem into smaller, more tractable problems. The approach adopted here was to decompose the wing optimization process into three separate, but sequential and iterative tasks. The process described in Fig. 2 was applied iteratively to the following three optimization problems:

1) In the first pass, the wing planform shape and spanwise loading are held fixed (an elliptic loading is initially assumed), and the wing sectional profiles are optimized, allowing the thickness-to-chord ratios to vary. In this pass, the profiles are optimized one at a time sequentially along the span.

2) In the second pass, the wing profiles and planform geometry are held constant, and the wing span loading is optimized (the wing loading is represented by a classical Fourier series limited to four coefficients, and these coefficients are used as design variables).

3) In the third pass, the wing profiles and spanwise loading are held constant, while the variables defining the wing planform are optimized.

At the end of the three passes, the scale factors used to compute the 2.5 g wing loading from the 1 g loading are updated with a full analysis of the latest flexible wing geometry. Throughout this process, it is very important to keep the lift coefficient constant within a tight tolerance to preclude the tendency of the optimizer to increase the L/D by simply increasing the C_L. This three-pass process is then

Table 1 Design variables, parameters, constraints, and objectives

Analytical descriptor	Category	Lower bound	Upper bound
13 shape function parameters for each airfoil (×7 airfoils)	Design variables	0.00	1.00
Airfoil thickness-to-chord ratios	Design variables	0.0800	0.500
Ref. wing aspect ratio	Design variable	6.00	15.0
Ref. wing quarter-chord sweep	Design variable	0.00 deg	40.0 deg
Relative outboard to inboard sweep	Bounded constraint	−10.0 deg	10.0 deg
Relative tip to break chords	Design variable	0.100	1.00
Wing span load distribution (defined by four Fourier coefficients)	Design variables	N/A	
Skin thickness	Design variable	0.080 in.	N/A
Stiffening ratio (A_{st}/A_{sk})	Bounded constraint	0.500	0.660
Minimum load intensity	Inequality constraint	5000 lb in.	N/A
Strain values	Bounded constraint	0.0020	0.0120
Cruise altitude	Parameter	Fixed value	
Cruise speed	Parameter	Fixed value	
MTOW	Equality constraint	N/A	
Cash operating cost	Objective function	Minimize	

repeated until the minimization of the objective function is sufficiently converged.

The results of this optimization are illustrated in Figs. 12b and 13–21. Figure 13 shows the evolution of the objective function (fuel weight required for a constant range mission) for this optimization. As shown, the entire optimization process was run for about 6000 function calls. The main pacing item in the procedure is the KTRAN analysis, and since a full aircraft (trimmed) solution takes about 90 s on an IBM P5-575 machine equipped with power 5 processors, the total process took approximately 6 days to complete.

An examination of the data shows that the performance improvement for this configuration comes from a 44% increase in the wing aspect ratio, a 2% decrease in wing average thickness, and improved wing profiles. The new wing has an aspect ratio of AR = 10.7 compared to 7.40 for the initial wing (Fig. 14 shows the evolution of the aspect ratio). Based on this large increase in the aspect ratio and reduction in wing thickness, one would expect that the structural weight of the new wing would be significantly greater

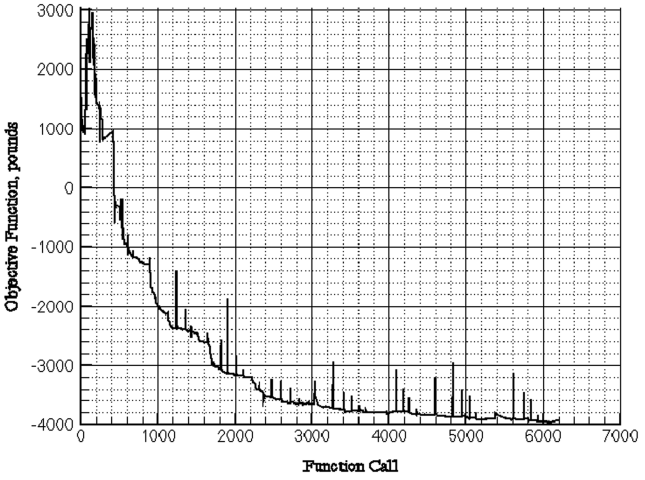

Fig. 13 Evolution of the objective function.

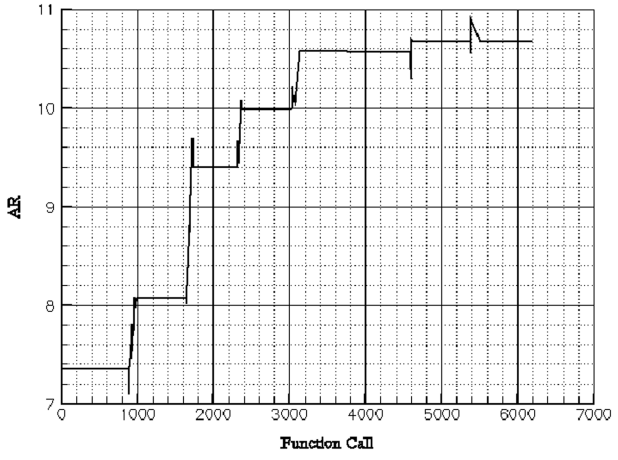

Fig. 14 Evolution of the reference wing aspect ratio.

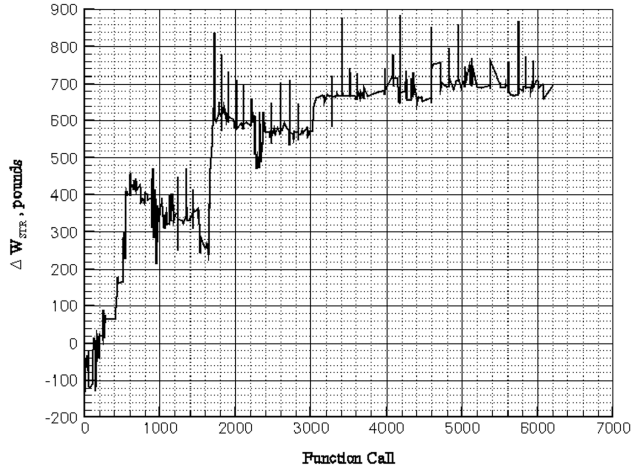

Fig. 15 Evolution of the structural mass.

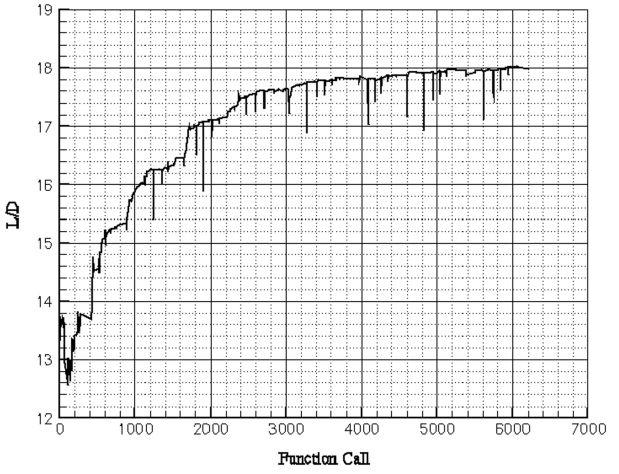

Fig. 16 Evolution of the lift-to-drag ratio.

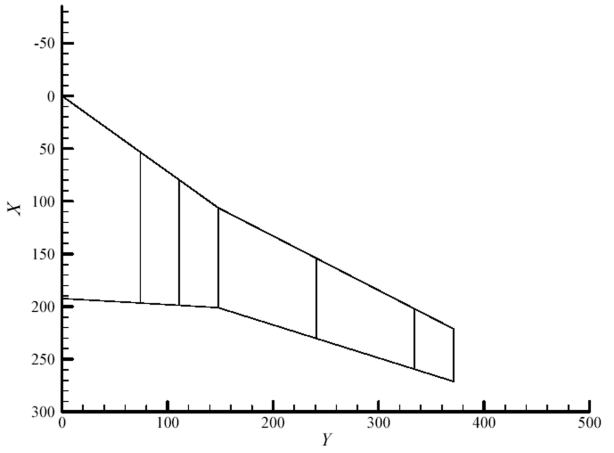

a) Wing planform before optimization

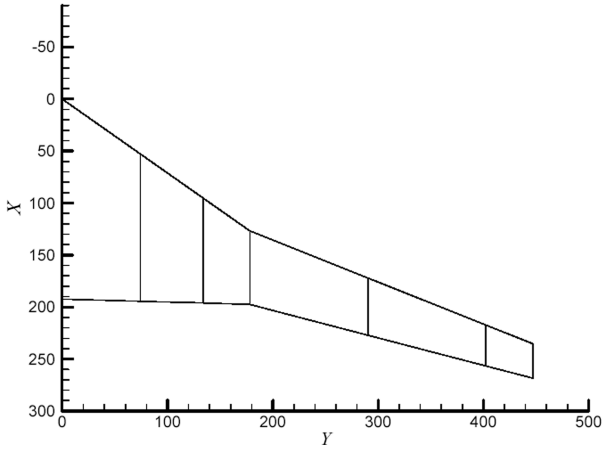

b) Wing planform after optimization

Fig. 17 Wing planform before and after aerostructural optimization.

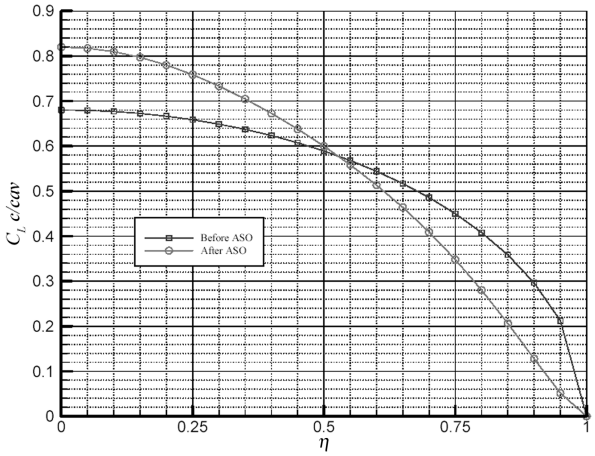

Fig. 18 Wing spanwise lift distribution before and after optimization.

considering the improvement in the L/D (Fig. 16). However, as shown in Fig. 15, the wing structural weight increased only by roughly 700 lb, or alternatively, 2.6% in BOW. The reason for this is that the optimizer compensated by reducing the wing sweep (by a 4.0 deg outboard of the planform break), by reducing the wing taper ratio (Fig. 17), and by shifting the wing loading significantly further inboard (Fig. 18). In the latter figure, the span load distributions include the winglet (i.e., $\eta = 0$ at the wing root, $\eta = 1$ at the winglet tip). This figure indicates that the optimizer not only shifted the load inboard to reduce the structural weight, but also to reduce trim drag by reducing the nose-down pitching of the wing, as well as generating more downwash at the tail, thereby increasing the tail thrust (as computed by KTRAN).

An interesting result is the fact that the optimizer chose to reduce sweep in favor of a 2% reduction in wing thickness, rather than the reverse choice, which was also plausible. It must be noted that the results presented here are only valid in the limited scope of the problem statement (i.e., only high-speed drag was considered, and only a one dimensioning load case was used), and only as accurate as the preliminary analysis codes employed. A postoptimality analysis with higher-fidelity tools is required to evaluate the actual performance improvements resulting from the optimization.

Figures 19–21 show the wing pressure distributions at three wing stations before and after the optimization. Note that the initial wing profiles used for this optimization were intentionally chosen to have poor aerodynamic characteristics to test the capability of the optimizer to improve the design. As shown, the optimization produced very benign, virtually shock-free pressure distributions.

IX. Conclusion

The development and application of a conceptual-preliminary aerostructural optimization capability was presented herein. In this approach, automated aerodynamic and structural analysis codes were developed and linked to the optimization environment and applied to the optimization of a business jet-type wing. A more realistic and robust composite objective function comprising a quasi-first principals based relationship between structures and

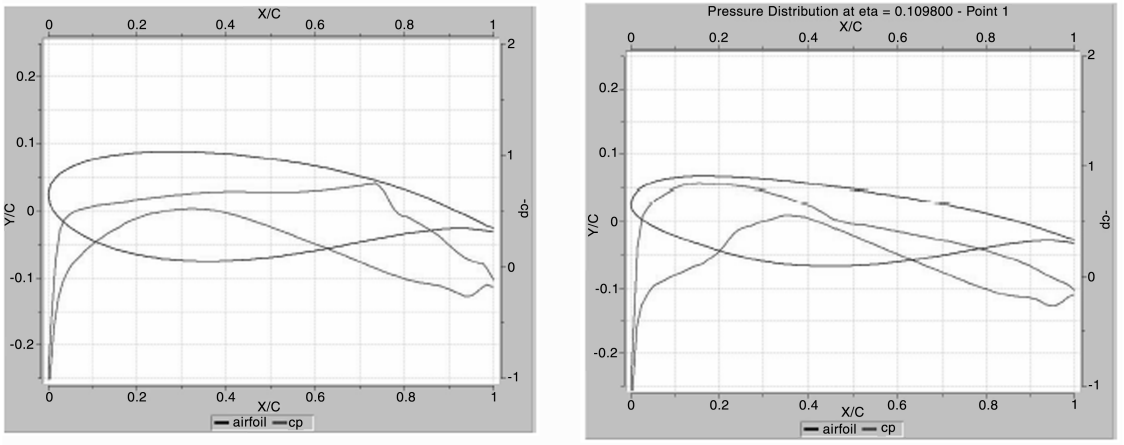

a) Before optimization **b) After optimization**

Fig. 19 Sectional pressure at $\eta = 0.109$.

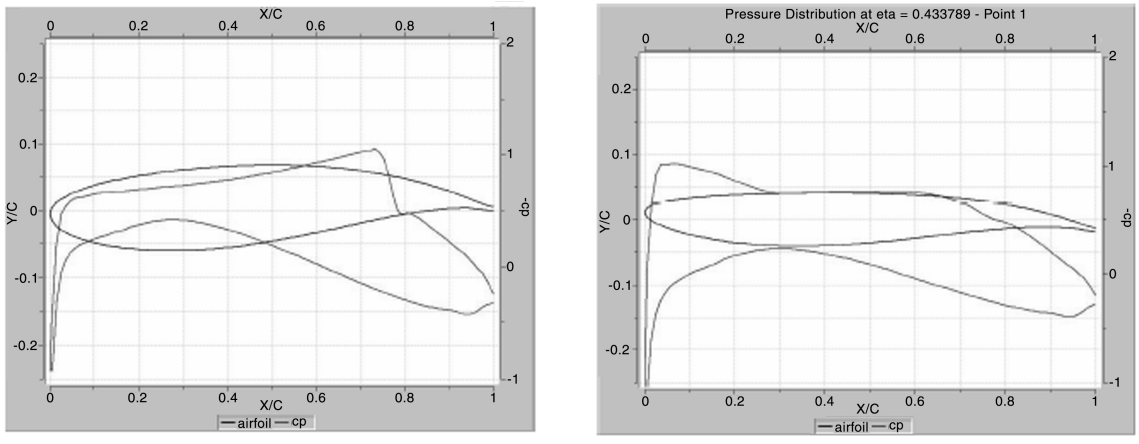

a) Before optimization **b) After optimization**

Fig. 20 Sectional pressure at $\eta = 0.400$.

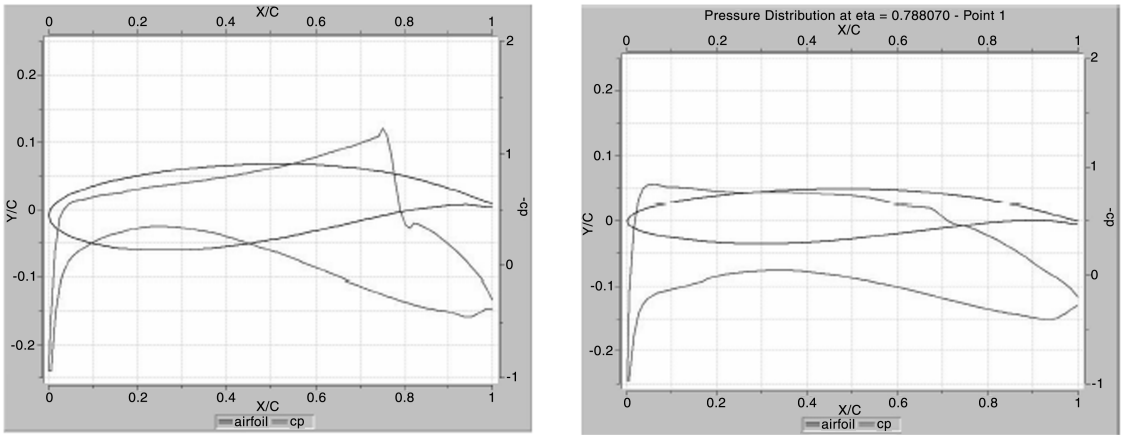

a) Before optimization **b) After optimization**

Fig. 21 Sectional pressure at $\eta = 0.800$.

aerodynamic attributes, and their combined effects on operating economics using fractional change functional transformations has been reviewed. The results presented here are preliminary in nature, but clearly illustrate the significant potential of an automated multidisciplinary optimization capability.

It is also shown that low-fidelity analysis codes, such as in this case a transonic small disturbance flow solver and a thin-wall structural analysis program, are very useful tools for the preliminary optimization of a complete aircraft. In combination with the closed-form algorithm for computing integrated operational performance, the speed of execution of these codes allows for the rapid investigation of numerous candidate designs in a practical time frame. As computer power continues to increase, higher-fidelity analysis codes will be incorporated in the multidisciplinary design optimization environment, while lower-order formulations will continue to be used in the conceptual-preliminary design environment to optimize configurations with an increasing number of design cases and constraints, thereby increasing the realism of the simulation.

Acknowledgments

Special acknowledgement is given to Alex van der Velden, David Vaughn, and David Kokan (formerly of Synaps, Inc.) for their help and collaboration in the initial stages of this project. The authors also want to acknowledge the collaboration of François Pépin, of the Advanced Aerodynamics Department of Bombardier Aerospace, in the initial development of the TWSAP program.

References

[1] Ashely, H., "On Making Things the Best-Aeronautical Uses of Optimization," *AIAA Aircraft Systems and Technology Conference*, AIAA, New York, Aug. 1981, pp. 1–32; also AIAA Paper 81-1738.

[2] Kafyeke, F., and Mavriplis, F., *CFD for the Aerodynamic Design of Bombardier's Global Express*, AIAA Paper 1997-2269, 1997.

[3] Goritschnig, G., Isikveren, A., Lamothe, M., and Munger, E., "The Evolution of Civil Aircraft Design at Bombardier: A Historical Perspective," *CASI Conference Proceedings*, [CD-ROM], Canadian Aeronautics and Space Institute, Ottawa, Toronto, 2003, pp. 1–14.

[4] Kroo, I., and Manning, V., "Collaborative Optimization: Status and Directions," AIAA Paper 2000-4721, 2000, pp. 1–11.

[5] Allwright, S., "Technical Data Management for Collaborative Multi-Discipline Optimization," AIAA Paper 96-4160, 1996.

[6] Sobieski, J., and Haftka, R. T., "Multidisciplinary Aerospace Design Optimization: Survey of Recent Developments," AIAA Paper 96-0711, 1996.

[7] Balling, R. J., and Wilkinson, C. A., "Execution of Multidisciplinary Design Optimization Approaches on Common Test Problems," *6th AIAA/NASA/ISSMO Symposium on Multidisciplinary Analysis and Optimization*, AIAA, Reston, VA, 1996, pp. 421–437; also AIAA Paper 96-4033-CP.

[8] Morris, A. J., and Gantois, K., "Combined MDO Optimization Including Drag, Mass and Manufacturing Information," *7th AIAA/USAF/ISSMO Symposium on Multidisciplinary Analysis and Optimization*, AIAA, Reston, VA, Sept. 1998, pp. 1724–1732; also AIAA Paper 98-4777.

[9] Van der Velden, A., Kelm, R., Kokan, D., and Mertens, J., "Application of MDO to Large Subsonic Transport Aircraft," AIAA Paper 2000-0844, 2000.

[10] Prandtl, L., "Applications of Modern Hydrodynamics to Aeronautics," translated as NACA Rept. 116 (original sources dated 1918–1920).

[11] Jones, R. T., "The Spanwise Distribution of Lift for Minimum Induced Drag of Wings Having Given Lift and Root Bending Moment," NASA TN-2249, 1950.

[12] Jones, R. T., and Lasinski, T., "Effect of Winglets on the Induced Drag of Ideal Wing Shapes," NASA TM-81230, 1980.

[13] McGeer, T., "Wing Design for Minimum Drag with Practical Constraints," *Journal of Aircraft*, Vol. 21, Nov. 1984, pp. 879–886.

[14] Craig, A., and McLean, J., "Spanload Optimization for Strength Designed Lifting Surfaces," AIAA Paper 88-2512, 1988.

[15] Wakayama, S., and Kroo, I., "Subsonic Wing Planform Design Using Multidisciplinary Optimization," *Journal of Aircraft*, Vol. 32, No. 4, July–Aug. 1995, pp. 746–753.

[16] Iglesias, S., and Mason, W. H., "Optimum Spanloads Incorporating Wing Structural Weight," *First AIAA Aircraft Technology, Integration, and Operations Forum*, AIAA, Reston, VA, Oct. 2001, pp. 1–10; also AIAA Paper 2001-5234.

[17] Grasmeyer, J. M., Naghshineh, A., Tetrault, P. A., Grossman, B., Haftka, R. T., Kapania, R. K., Mason, W. H., and Schetz, J. A., "Multidisciplinary Design Optimization of a Strut-Braced Wing Aircraft with Tip-mounted Engines," MAD Center Rept. MAD-98-01-01, Jan. 1998.

[18] Giesing, J. P., and Wakayama, S., "A Simple Cost Related Objective Function for MDO of Transport Aircraft," *35th Aerospace Sciences Meeting and Exhibit*, AIAA, Reston, VA, Jan. 1997, pp. 1–14; also AIAA Paper 97-0356.

[19] Johnson, V. S., "Minimizing Life Cycle Cost for Subsonic Commercial Aircraft," *Journal of Aircraft*, Vol. 27, No. 2, Feb. 1990, pp. 139–145.

[20] Samareh, J. A., "Aerodynamic Shape Optimization Based on Free-Form Deformation," *10th AIAA/ISSMO Multidisciplinary Analysis and Optimization Conference*, AIAA, Reston, VA 30 Aug.–1 Sept. 2004.

[21] Jameson, A., Shankaran, S., Martinelli, L., Haimes, B., "Aerodynamic Shape Optimization of Complete Aircraft Configurations Using Unstructured Grids," *42nd Aerospace Science Meeting*, AIAA, Reston, VA, 2004, pp. 1–14; also AIAA Paper 2004-0533.

[22] Martins, J. R., Alonso, J., and Reuther, J., "A Coupled-Adjoint Sensitivity Analysis Method for High-Fidelity Aero-Structural Design," *Optimization and Engineering*, Vol. 6, No. 1, March 2005, pp. 33–62.

[23] Chiba, K., Obayashi, S., Nakahashi, K., and Morino, H., "High-Fidelity Multidisciplinary Design Optimization of Aerostructural Wing Shape for Regional Jet," AIAA Paper 2005-5080, June 2005.

[24] Obayashi, S., Oyama, A., and Nakamura, T., "Transonic Wing Shape Optimization Based on Evolutionary Algorithms," *High Performance Computing*, Third International Symposium, ISHPC 2000, edited by M. Valero, K. Joe, M. Kitsuregawa, and H. Tanaka, Springer–Verlag, Berlin, Oct. 2000.

[25] Isikveren, A., "Parametric Modeling Techniques in Industrial Conceptual Transport Aircraft Design," SAE Paper 2003-01-3052, Sept. 2003.
[26] General Aviation Synthesis Program-GASP, NASA CR-152303, Cosmic Program ARC-11434, 1978.
[27] Abdo, M., Piperni, P., Isikveren, A., and Kafyeke, F., "Optimization of a Business Jet," *Canadian Aeronautics and Space Institute Annual General Meeting, Aircraft Design & Development Symposium*, [CD-ROM], Canadian Aeronautics and Space Institute, Ottawa, Toronto, April 2005.
[28] Abdo, M., L'Heureux, R., Pépin, F., and Kafyeke, F., "Equivalent Finite Element Wing Structural Models Used for Aerodynamics-Structures Interaction," *CASI 16th Aerospace Structures & Materials Symposium*, [CD-ROM], Canadian Aeronautics and Space Institute, Ottawa, Toronto, 2003.
[29] Chintapalli, S., Sedaghati, R., Li, J., and Abdo, M., "Minimum Mass Design of Stringer Stiffened Compression Panels Under Compressive Axial Load," WCSMO6 Paper 2005-1671, May 2005.
[30] Reymond, M., and Miller, M., MSC/NASTRAN, *Quick Reference Guide*, Ver. 68, 1994.
[31] Kafyeke, F., and Piperni, P., "Applications of KTRAN Transonic Small Disturbance Code to the Challenger Business Jet Configuration with Winglets," SAE Paper 881483, Oct. 1988.
[32] Piperni, P., and Kafyeke, F., "Applications of the KTRAN Transonic Small Disturbance Code to the Complete CF-18 Aircraft with Stores," *Canadian Aeronautics and Space Institute (CASI) Journal*, Vol. 36, No. 3, Sept. 1990, pp. 153–165.
[33] Piperni, P., Patel, K., and Kafyeke, F., "The Prediction of Aircraft Trim Drag in Transonic Flight Using CFD," *46th Annual CASI Conference, Montreal*, [CD-ROM], Canadian Aeronautics and Space Institute, Ottawa, May 1999.
[34] Hoerner, S. F., *Fluid Dynamic Drag*, Hoerner Fluid Dynamics, Brick Town, NJ, 1965.
[35] Lock, R. C., "Prediction of the Drag of Wings at Subsonic Speeds by Viscous/Inviscid Interaction Techniques," AGARD Rept. 723, 1985.
[36] Munk, M., "The Minimum Induced Drag of Airfoils," NACA, Rept. 121, 1921.
[37] Kuhn, P., Peterson, J., and Levin, L., "A Summary of Diagonal Tension, Part 1—Methods of Analysis," NACA Technical Note 2661, 1952.
[38] Burt, M. E., "Weight Prediction for Wings of Box Construction," RAE Report No. Structures 186, 1955.
[39] Shanley, F. R., *Weight-Strength Analysis of Aircraft Structures*, Dover Publications Inc., New York, 1960.
[40] Farrar, D. J., "The Design of Compression Structures for Minimum Weight," *Journal of the Royal Aeronautical Society*, Vol. 2, Nov. 1949, pp. 1041–1052.
[41] Isikveren, A., "Identifying Economically Optimum Flight Techniques of Transport Aircraft," *Journal of Aircraft*, Vol. 39, No. 4, July–Aug. 2002, pp. 528–544.
[42] Torenbeek, E., *Synthesis of Subsonic Airplane Design*, Kluwer Academic Publication, Norwell, MA, 1988.
[43] Torenbeek, E., "Optimum Cruise Performance of Subsonic Transport Aircraft," Delft University of Technology, Rept. LR-787, Faculty of Aerospace Engineering, The Netherlands, March 1995.